

Developing a Line-scanning Hyperspectral Imaging System for Monitoring Plant Status



UNIVERSITY OF
LINCOLN

James Bennett

School of Computer Science

College of Science

University of Lincoln

Submitted in partial satisfaction of the requirements for the
Degree of MSc Robotics and Autonomous Systems
in Computer Science

Supervisor Dr. Junfeng Gao

September 2022

Abstract

In this project, an automated hyperspectral imaging (HSI) system is built for monitoring plant status. There is an increasing trend toward the adoption of precision agriculture technologies which rely on insights from timely monitoring of crops to action intervention that aids in the plant's growth. HSI is adopted for monitoring crops by remote sensing but not for close-range individual plant monitoring. A Specim FX10 hyperspectral line scanning camera is mounted to a custom linear actuator and controlled via a web interface. Crops are imaged in situ which requires accommodating variance in natural illumination. A pipeline has been built to correct for these variances using a white reference panel in each image and prepare the data for analysis. Supplementary artificial illumination was added using 4 x 50 W halogen reflector bulbs that move with the camera but limitations were found and alternative suggestions made. The health of the plant is determined using spectral features of individual pixels with an SVM classifier. The system was validated on potatoes grown in pots in a polytunnel and was able to distinguish between plants that were given fertiliser and those that hadn't with 68.5% accuracy.

List of Tables

4.1	Initial risk assessment.	26
4.2	Revised risk assessment.	28
5.1	Pugh Matrix for selecting drive type.	36
5.2	Table giving scale invariant similarity error scores as per Equation 5.2 for different illumination variations.	46
6.1	Table comparing the health assessment of each plant against its label.	61
6.2	Table giving classification accuracy for different data configurations. .	65

List of Figures

2.1	Example hyperspectral image of green leaf. (a) Data cube comprised of stack of narrow band sub images (only some shown); (b) reflectance spectrum of a pixel. Source Mishra, Asaari et al., 2017.	5
2.2	Illustration of smile and keystone aberration effects. Source Specim, n.d.	9
3.1	The systems vee approach to development.	13
3.2	Risk matrix used for assessing risk level.	18
4.1	A structural SysML block definition diagram modelling the system context.	20
4.2	A structural SysML block definition diagram modelling the subsystem decomposition.	22
4.3	Structural SysML block definition diagram for the final system design.	29
5.1	Types of halogen lamp. Images from Lightbulbs Direct, 2022	32
5.2	Example configuration of 4 narrow angle lamps in an array.	33
5.3	Example configuration of 2 wide angle lamps in an array.	34
5.4	A render from the CAD model showing the lighting configuration and positioning.	35
5.5	Specification of MGN rail.	37
5.6	Fusion 360 CAD model of part of the linear actuator.	38
5.7	The built version of the linear actuator.	39
5.8	A photo of the main electrical system.	41
5.9	A photo of the circuit board built for controlling the actuator.	42
5.10	Raw image of sample plant using R = 650 nm, G = 530 nm and B = 466 nm.	44
5.11	Spectral signatures of pixels from different parts of the image in Figure 5.10.	45
5.12	Spectral signatures of pixels from the white reference panel under different illumination environments.	46

5.13 Reflectance calibrated image of sample plant using R = 650 nm, G = 530 nm and B = 466 nm.	49
5.14 Spectral signatures of pixels from different parts of the image in Figure 5.13.	50
5.15 Spectral signatures of pixels from different parts of the image in Figure 5.13.	51
5.16 Spectral signatures of pixels from calibrated images of plants under different illumination.	51
5.17 Image of the Ratio Vegetation Index applied.	53
5.18 Image after thresholding and erosion.	54
 6.1 Photo of system during testing.	62
6.2 Two types of imaging artefact that void a scan.	63
6.3 Confusion matrices for classification on classes NF and BF with no artificial illumination.	64
6.4 Confusion matrices for classification on classes NF and BF with artificial illumination set to full.	64
6.5 Confusion matrices for classification on classes NF, BF and TD with artificial illumination set to full.	65

List of source codes

1	Code snippet of reflectance retrieval	48
2	Code snippet of leaf extraction.	52
3	Complete processing pipeline	56

Table of Contents

1	Introduction	1
1.1	Aim	1
1.2	Objectives	1
1.3	Motivation	2
2	Literature Review	4
2.1	Hyperspectral Imaging Fundamentals	4
2.2	Potato Crop	4
2.3	Acquisition	5
2.3.1	Camera	5
2.3.2	Motion	6
2.3.3	Illumination	7
2.3.4	Calibration	8
2.4	Processing	10
2.4.1	Reflectance Retrieval	10
2.4.2	Spectral Smoothing	11
2.4.3	Segmentation Masking	11
2.4.4	Feature Selection	12
2.5	Analysis	12
3	Methodology	13
3.1	Development Approach	13
3.2	Evaluation Methodology	15
3.3	Project Management	15
3.3.1	Project Constraints	15
3.3.2	Time Management	16
3.3.3	Risk Management	17
4	System Design	19
4.1	Understanding the System Context	19
4.2	System Decomposition	21

4.2.1	Acquisition	22
4.2.2	Processing	24
4.3	Feasibility	26
4.4	Final System Design	28
5	Development	30
5.1	Acquisition Subsystem Development	30
5.1.1	Camera	30
5.1.2	Illumination	30
5.1.3	Linear Actuator	35
5.1.4	Control	39
5.1.5	Electrical	41
5.1.6	Cart	42
5.2	Processing Subsystem Development	43
5.2.1	Correction	43
5.2.2	Pre-processing	52
5.2.3	Analysis	54
6	System Validation	60
6.1	Procedure	60
6.2	Results	62
7	Discussion	66
7.1	Creating an automated acquisition system	66
7.2	Developing a processing pipeline	68
7.3	Investigating algorithms for health classification	69
7.4	Validation of the system	69
7.5	Personal Reflection	70
8	Conclusions	72

Chapter 1

Introduction

1.1 Aim

This project aims to develop an automated hyperspectral imaging system for monitoring plant status. The outcome will be a system which automatically images the plant and performs processing and analysis on the image. The imaging system will be mobile such that it can be taken to plants at their location, performing in-situ non-invasive scans rather than disturbing plants by moving them or taking samples from them in a destructive way. Automated analysis will be performed on the images to give timely insights into the plant's health status facilitating targeted interventions.

1.2 Objectives

The objectives that will lead to the aim being realised are:

- Create an automated acquisition system that will capture hyperspectral images of the plant's canopy.
- Develop a processing pipeline to extract and fuse spectral and image-level features from the images for plant monitoring.
- Investigate advanced machine learning algorithms for potato plant classification of health.
- Validate the system on potatoes grown in a polytunnel.

These objectives will be used in evaluating the outcome of the project.

1.3 Motivation

The agricultural sector is facing several challenges, putting global food production under increasing pressure. These challenges include: a growing population, leading to increased demand for food; climate change bringing pressure to decarbonise food production and cope with more varied and extreme weather conditions; increasing regulation that limits crop management options; increasing costs of production contributing to reduced profit margins; deficient labour availability and a changing skill-set of the workforce.

Precision agriculture offers technologies to aid in mitigating these challenges. The aim of precision agriculture is the use of monitoring and intervention techniques that improve efficiency. These are delivered through the use of sensing technologies and automation (Duckett et al., 2018).

Crucial to this approach is automation. Firstly, automation removes the time burden which helps ensure that tasks get done, secondly, it also removes the technical burden of monitoring and ensures tasks are completed with consistent accuracy. Another beneficial aspect automation brings is the ability to collect and comprehend vast amounts of data which affords the ability to monitor plants individually and treat them at a sub-field scale - or even at a per-plant scale - rather than at a farm scale. To deliver such targeted interventions it is wholly necessary to have suitable sensing technologies that deliver appropriate insights. It should be noted that if insights are to be gathered at a per-plant level then destructive testing is a fundamentally flawed methodology.

There is significant interest and effort being put into solutions to automate plant health monitoring. At the commercial end, solutions are being offered using drone imagery , aerial imagery, and environmental sensors. Toward the early development end, there is interest in genetically engineering plants to report their health, electro-chemical sensors attached to plants, and imaging including with RGB, thermal and indeed hyperspectral technologies (Roper, Garcia and Tsutsui, 2021).

Hyperspectral imaging (HSI) is the combination of *point spectroscopy* and *imaging*.

Spectroscopy is the study of how light interacts with materials, offering a spectral signature and imaging provides the information on where that spectral signature is located in the spatial domain. Different wavelengths of light across the electromagnetic spectrum interact with different materials differently which yields the spectral signature. This insight into the spectral composition of a scene can reveal differences between two objects that can be imperceptible to the human eye.

Hyperspectral imaging currently sees uses in several applications (Khan et al., 2018). In the medical field, HSI is an emerging imaging modality, especially for disease diagnosis and image-guided surgery (Lu and Fei, 2014). HSI sees applications in military and surveillance for identifying objects and patterns that are indistinct to the human eye (Yuen and Richardson, 2010). In the waste management industry, the technology is used to identify different materials, especially different types of plastic for sorting (Serranti, Gargiulo and Bonifazi, 2011). Within the agricultural domain, HSI is used in plant phenotyping, that is measuring characteristics or traits of a plant in order to be used for breeding and engineering new varieties (Sarić et al., 2022). It is also used widely in food processing to monitor the quality of meat, the freshness of fruit, and to identify defects. HSI is also gaining increasing traction within the precision agriculture space, with new advances making possible the evaluation of crop stresses, analysing soil and vegetation characteristics (Khan et al., 2018) with Sarić et al. (2022) acknowledging the potential but also the challenges of affordable, in-field HSI devices.

HSI has proven itself in many applications for discerning differences in materials not visible to the human eye and has proven itself for discerning differences between plants. However, the majority of HSI plant imaging systems are lab based and the goal here is to develop a system that will image the plant *in situ*, in the field, to reveal insights about the plant's health as it grows to facilitate timely action in line with the goals of precision agriculture.

Chapter 2

Literature Review

2.1 Hyperspectral Imaging Fundamentals

When light interacts with an object, different wavelengths of the electromagnetic spectrum are reflected in different intensities (Gates et al., 1965; Paulus and Mahlein, 2020). These vary according to factors such as the leaf structure, biochemical composition, chlorophyll presence, water content. Spectroscopy is the method of acquiring the spectral signature of an object whereby the intensity of different wavelengths of light is measured. Hyperspectral imaging (HSI) combines this modality with imaging which yields data containing both spectral and spatial information. The output of HSI is a 3D datacube which is a series images for a narrow wavelength band across the reflectance spectrum; Mishra, Asaari et al. (2017) illustrate this in Figure 2.1(a) showing the datacube as a stack of narrow band images and Figure 2.1(b) as an example spectral signature for one pixel.

2.2 Potato Crop

Potato is a staple of many societies worldwide and its production occurs in many regions of the UK. Growers face several challenges (Halley and Soffe, 2003) including diseases such as blight which can devastate potato crops and must be managed closely, stresses from soil conditions, pests or drought which is of particular concern in coastal areas exposing potato crops to salt stress (Aghaei, Ehsanpour and Komatsu, 2008). There have been several examples of studies which look at the

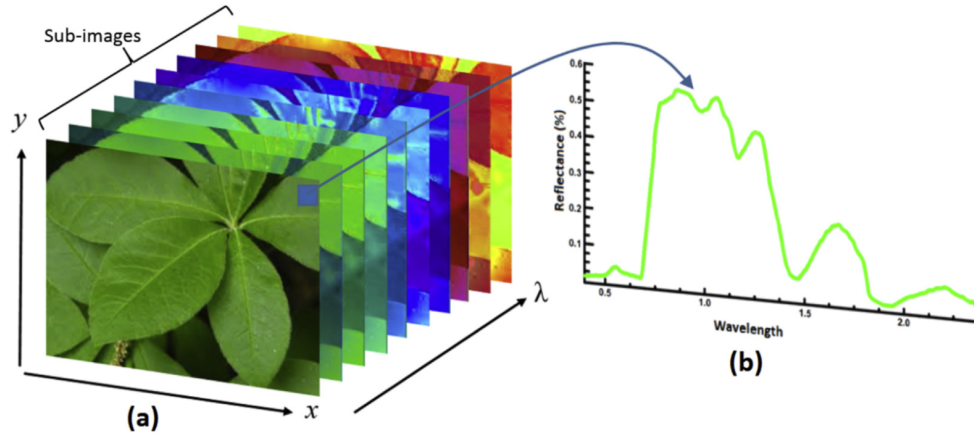


Figure 2.1: Example hyperspectral image of green leaf. (a) Data cube comprised of stack of narrow band sub images (only some shown); (b) reflectance spectrum of a pixel. Source Mishra, Asaari et al., 2017.

spectral reflectance of potato plants to address the challenges. Some of these are: water stress detection using HSI and other modalities (Gerhards et al., 2016); disease detection using contact spectroscopy of blight (Gold et al., 2020; Couture et al., 2018); and in-field early-blight detection using HSI in an enclosed rig with artificial lighting (Van De Vijver et al., 2020). These studies add to the confidence that HSI of potato plants will yield valuable insights but they do not present a working system meeting the requirements.

2.3 Acquisition

2.3.1 Camera

Hyperspectral images commonly have hundreds of spectral bands, therefore, acquisition of the 3D data cube with a 2D sensor array poses challenges which do not exist in the same way for conventional capture, such as for an RGB camera or even multispectral camera (<20 bands). Mishra, Asaari et al. (2017) outline the four main approaches to acquiring the datacube.

- **Point scanning** (whisk-broom) where the complete spectrum is acquired sequentially for each point across both spatial dimensions. This method takes a long time and requires accurate motion control in two dimensions.

- **Line scanning** (push-broom) where the spectra of a line of pixels is acquired simultaneously and the camera is moved in one spatial dimension. The light entering the lens is dispersed into its colours over the 2D sensor array. This method can suffer from motion artefacts but to a lesser extent than point scanning and calibration is required to avoid striping.
- **Area scanning** (spectral scanning) where a 2D image for a particular wavelength is captured at a time, usually achieved using band pass filters. This method can suffer from spectral smearing and a reduced number of bands.
- **Snapshot imaging** (non-scanning) captures spatial and spectral information simultaneously. These are considerably faster and avoid motion artefacts but these devices are still in an early stage of development.

For this work, a line scanning camera was available, deemed appropriate and is most widely used in plant phenotyping (Paulus and Mahlein, 2020). Specifically, the Specim FX10 line scanning camera¹ will be used. The camera operates in the 400 - 1000 nm range (visible plus near infrared) with a spectral resolution of 224 bands and a spatial resolution of 1024 px.

2.3.2 Motion

Since a line scanning camera is being used, relative motion between the plant and camera must be generated along one axis. There are two options: move the sample or move the camera. Due to the impracticalities of moving potato plants onto a moving platform, the system will move the camera. Of the automated systems surveyed a linear actuator was a choice (Morales et al., 2022) which offers precise control in a singular package requiring low build requirements, however, these are expensive and come in a limited set of sizes. Details are sparse for other aspects of the design such as what the equipment is mounted to, the control algorithms and whether the motion is constrained with linear glides, wheel and track systems or otherwise.

An alternative approach could be a belt driven actuator such as the kit² available

¹<https://www.specim.fi/products/specim-fx10/>

²<https://ooznest.co.uk/product/belt-driven-linear-actuator-kit>.

from Ooznest. The stepper motor turns a timing pulley, driving a belt connected to a carriage which moves linearly along the length of aluminium extrusion. Various items can be mounted to the carriage. The stepper motor is readily controlled by a driver and Arduino with drivers available. With 8x microstepping employed, the theoretical precision is 0.0375 mm and the test data by the company, Ooznest Limited (n.d.) show a repeatability of 0.238 mm and accuracy of 0.260 mm once the effects of the transmission and roller systems have been accounted for. A further benefit of this system is that it can be customised for any length desired.

The required speed of the relative motion is determined by the camera frame rate, exposure time, field of view and height above sample (Paulus and Mahlein, 2020). The correct speed determined by Equation 2.1 and calibrated using the procedure in Section 2.3.4.

$$speed = FPS * \frac{2 * h * \tan \frac{\alpha}{2}}{w} \quad (2.1)$$

where FPS is the camera frame rate, h is the distance above the sample, α is the field of view of the camera, and w is the number of spatial pixels along the line scan.

The imaging will occur from above the plant looking down onto the canopy therefore the size and height of the plant must be considered. The factors leading to this decision include the resolution, field of view, lens and plant height (Paulus and Mahlein, 2020). If time series data is to be captured, the height of the camera should be adjustable to accommodate plant growth and ensure the canopy remains in focus.

2.3.3 Illumination

Illumination is a critical consideration for HSI since the reflectance is the focus of the measurement. Many examples seek to create an enclosure to exclude any external illumination and add artificial illumination inside (Zhang et al., 2019; Van De Vijver et al., 2020; Morales et al., 2022). Mostly, halogen lamps are used for artificial illumination since they are a broad band emitter and affordable. LEDs or fluorescent

tubes are unusable because they emit high narrow bands of the spectrum (Paulus and Mahlein, 2020). The benefits of artificial illumination are the light is constant during the course of a capture and from one day to another significantly reducing image artefacts and calibration requirements. There are disadvantages with artificial illumination such as heat stress on the plants, although this could be solved with optical fibres such as in Zhang et al. (2019); Mishra, Asaari et al. (2017) explain that in artificial illumination the top leaves of a plant receive more illumination than the bottom which requires complex correction; and in a portable system it can be particularly difficult to exclude external light. Paulus and Mahlein (2020) claim the use of passive light, such as sunlight is preferable but that calibration routines are required for accurate reflectance values.

2.3.4 Calibration

It has already been said in this paper that calibration is important in both spatial and spectral dimensions. There are many calibration methods covered in literature; the following papers provide good coverage (Paulus and Mahlein, 2020; Morales et al., 2022; Van De Vijver et al., 2020; Mishra, Sytsma et al., 2022). During the research, the calibration methods they present will be used to either verify an aspect is already calibrated or to perform the calibration where necessary.

Optical aberration. Effects such as smile and keystone are common in pushbroom cameras (Morales et al., 2022) and are caused by the camera optics. As illustrated in Figure 2.2, keystone causes spatial distortions and smile causes spectral distortions. Fortunately, the Specim cameras contain hardware correction algorithms to overcome these aberrations (Specim, n.d.) and Morales et al. (2022) present methods of verifying the calibration. For keystone a horizontal line is captured and analysed and for smile, a target of known reflectance is placed in different parts of the image and analysed.

Spectral response. As the spectra is spread out over the array and captured into bins, specific wavelength bands must be assigned to each bin. This process

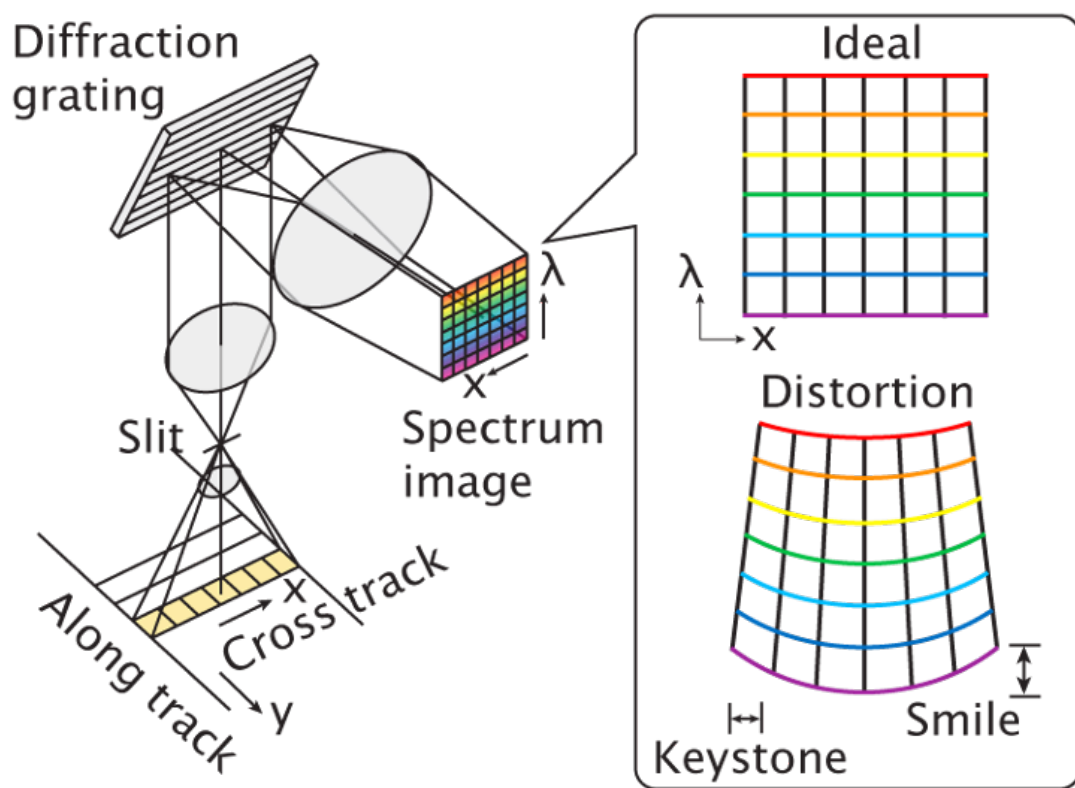


Figure 2.2: Illustration of smile and keystone aberration effects. Source Specim, n.d.

involves advanced equipment and is performed by the manufacturer. By capturing the spectral response of a Zenith polymer with a known spectral signature it is possible to verify the spectral response of the camera (Morales et al., 2022).

Morphological correction. In Section 2.3.2, Equation 2.1 was given to calculate the speed, however errors in measurement can lead to the true speed being different to the calculated one. Popular calibration techniques involve putting a checkerboard pattern or circular disc in the image frame Mishra, Sytsma et al., 2022; Morales et al., 2022. The image is captured, masked then squares or ellipses are fitted to the objects. The longest and shortest axes are identified and any corrections made to the scanning speed and the process repeated for verification.

2.4 Processing

2.4.1 Reflectance Retrieval

In its raw form, the data captured is *radiance data* which is an absolute measurement and cannot be used without calibration. Instead, it is often preferred to use reflectance data (Paulus and Mahlein, 2020) which is possible if the spectral composition of the illumination source is known. This can be acquired using a digital device or by placing a white reference panel in the image which is certified to reflect all wavelengths above 99%. Using reflectance is also desirable since the output HSI is normalised to different illumination conditions which readily allows for the comparison of different images.

Equation 2.2 is used to obtain the reflectance image Morales et al., 2022,

$$I_{reflectance} = \frac{I_{raw} - I_d}{I_w - I_d} \quad (2.2)$$

where I_{raw} is the captured image, I_d is the dark reference image which is obtained when the camera shutter is closed, and I_w is the white reference image which is a material that reflects the incoming radiation with known a spectral signature.

Paulus and Mahlein (2020) caution that for measurement in variable conditions,

such as a greenhouse, it is recommended to use multiple white reference panels in an image or to perform periodic recalibration.

2.4.2 Spectral Smoothing

HSI tends to produce noisy data in the spectral domain because there are a lot of narrow bands (Zhang et al., 2019). It may also contain anomalies from dead pixels showing permanently black or spikes where the spectrum has a sharp rise and decline (Mishra, Asaari et al., 2017). It is appropriate to assume the plant spectrum is smooth and that sharp peaks are the result of outliers and noise thus a soft smoothing algorithm may be applied (Paulus and Mahlein, 2020).

There are conflicting claims in the literature as to the best algorithm to use. For example, Paulus and Mahlein (2020) state the Savitzky-Golay smoothing algorithm (Guiñón et al., 2007) is most established for HSI. However, Zhang et al. (2019) say the wavelet transform (Roy et al., 2000) is particularly suited to HSI due to the non-linear and non-stationary signal. These two methods alongside a simple moving average (Guiñón et al., 2007) will be considered during this research.

2.4.3 Segmentation Masking

To find regions of interest within the image to perform analysis on, the image must be segmented into groups. The primary goal is extracting leaves from the background which will likely be performed in the spatial domain with colour thresholding and erosion to clean the image (Paulus and Mahlein, 2020). Selection of a particular wavelength can aid discriminating background from foreground (Zhang et al., 2019). If further segmentation of particular leaves is desirable then a machine learning (ML) method can be employed for this (Paulus and Mahlein, 2020). Spectral segmentation is possible but is rarely employed and considered to be more of an analytical tool than a masking technique (Mishra, Asaari et al., 2017).

2.4.4 Feature Selection

Due to the vast amounts of data in the 3D datacube, it often contains redundant information and in most cases can be represented in fewer latent variables which will aid in prediction (Mishra, Asaari et al., 2017). Feature *selection* involves eliminating redundant features by selecting a subset of features that discriminate most whilst maintaining reconstruction ability. Zhang et al. (2019) demonstrate the successive projections algorithm, extracting the 6 most important spectral features which were passed to a ML classifier. Feature *extraction* involves creating a new set of features by transforming the data into a new feature space; a common approach is principle component analysis (Mishra, Asaari et al., 2017). The nature of the best set of features will depend on the data, the focus of the analysis and the methods employed so these approaches will be investigated further during the course of the research.

2.5 Analysis

To validate the performance of the system, analysis will be conducted on data acquired. For data such as HSI, ML is a valuable tool and widely used throughout the literature, especially since it is a multivariate problem (Mishra, Asaari et al., 2017). Since we know the conditions the potatoes will have been exposed to, the analysis lends itself to a supervised learning problem. The problem will be more formally defined during the research as work is conducted alongside plant scientists and other specialists as they observe the potato plants. It must also be decided whether to formulate the problem as a classification or regression problem. Some learning methods identified in literature (Zhang et al., 2019; Paulus and Mahlein, 2020; Mishra, Asaari et al., 2017) include random forests, support vector machine, neural network architectures and linear discriminant analysis for classification. Or for regression methods such as support vector regression, partial least squares and binary logistic regression. The suitability of these methods will be considered in view of the data and problem definition.

Chapter 3

Methodology

3.1 Development Approach

To structure the approach to developing a solution, the systems vee process Figure 3.1 was utilised. This process helps to ensure the right system is built and the system is built right.

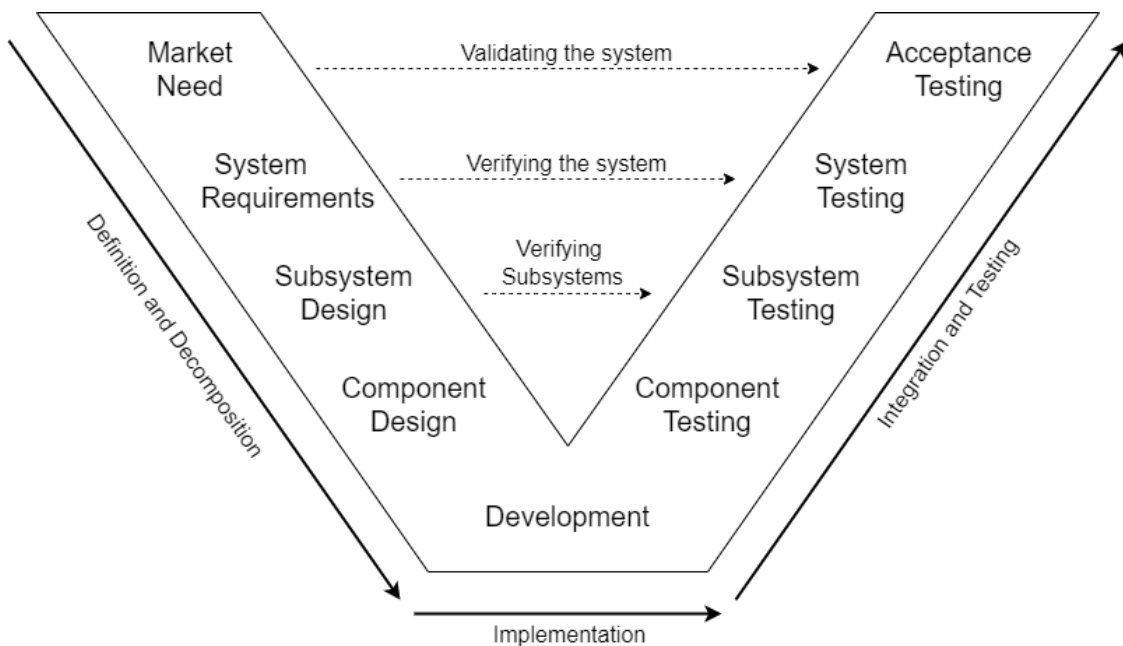


Figure 3.1: The systems vee approach to development.

The process begins at the left hand side of the vee and entails defining the problem and needs of the system before decomposing it into suitable subsystems, and in turn components, creating smaller and more manageable pieces. Across the bottom of the diagram, individual components are designed, built and tested. On the right

hand side, the built components and subsystems are integrated and tested before performing full system verification and validation. At any level of the integration and testing, if the requirements aren't sufficiently met, it is possible to iterate, travelling back to the left half to re-design, re-implement and re-test a particular component or subsystem of the solution. In following this process, the emphasis is moved away from the implementation and put on the definition, decomposition and testing to aid in ensuring a solution is delivered which is fit for purpose.

Throughout the project, SysML will be used as a tool. SysML is a graphical language that is used for modelling systems and is particularly useful for describing the structure and behaviour of complex systems. SysML is well suited to interdisciplinary projects such as this, able to combine hardware, software and abstract elements under one language. On the structural side of SysML, it will be used during the requirements capture and decomposition into subsystems by understanding where this solution fits into the wider context and how the subsystems are required to interact with each other and their environment. The behavioural aspect of SysML is more appropriate during the component design, especially for user interactions and software and control elements. SysML is a useful tool that can define a design such that it provides a reference that can be used to test against and that can be used to concisely and effectively communicate, hence its use in this report. It should be noted that SysML is used to *model* systems and as such the models are a simplification of real life, but a necessary simplification in order to understand, represent and address the problem.

Several other tools have been used for the development of this project. Autodesk Fusion 360 was used for mechanical Computer Aided Design (CAD). Creating a mechanical model in CAD helps to eliminate issues in design rather than integration where it is much cheaper and has much less impact on the project's timeline. Visual Studio Code IDE was used for all the programming including the Arduino code, web pages and data processing scripts. Version control is a critical aspect of any project and thus tools were used to implement it. GitHub was used for version control on the software and Fusion 360's integrated version to manage the CAD designs.

3.2 Evaluation Methodology

The systems vee model helps encourage proper testing, helping to ensure a system is developed that is fit for purpose. As each component is built it will be tested against the specification which will identify deficiencies before they are integrated. As the components are brought together into their subsystems tests will be conducted on the function of the subsystem to ensure it functions as specified and identify any integration challenges in components. It may only be at this stage that it is realised the design was lacking a feature to meet an element of the specification in which case, the design will have to be iterated.

To perform final validation of the complete system, an experiment will be conducted, imaging potato plants, processing them and analysing them to gain insights into their health.

3.3 Project Management

Work for this project began in April 2022 when a brief of the project was discussed in an initial meeting with the key stakeholders. Those included Prof Erik Alexandersson of the Swedish University of Agricultural Sciences, a plant scientist who has some experience with conventional imagery of potatoes and hyperspectral imagery and has lent the camera; Dr Iain Gould, a plant and soil scientist at the University of Lincoln; Dr Junfeng Gao, my supervisor; and myself. Following the brief, time was spent researching the problem domain and developing a project proposal. Between the proposal and the start of the project in July the project was refined in conjunction with my supervisor and important stakeholders such as the engineering workshop and crop specialists to understand the facilities and resources available and any constraints for the project.

3.3.1 Project Constraints

Before beginning the development of this project it is important to understand any constraints.

Time. The deadline for the project is 22nd September 2022. The project time commenced on the 20th June 2022 but with other commitments during that period approximately 10 weeks to work on the project were available.

Deliverables. In addition to the project artefact, a requirement is to deliver this report and a poster before the deadline.

Finance. A limit was not set on the budget but it was decided costs should not be excessive and that cost-effectiveness was important. The design was presented to and discussed with the project supervisor for approval.

Subject crops. The systems needed to be validated on a subject crop therefore one must be sourced. Dr Iain Gould provided access to trials of crops growing at the University of Lincoln Riseholme campus.

Skill and expertise. Whilst this is a research project and new areas and avenues will be explored, the project should best utilise my existing skill set and help me to develop new ones, acknowledging this is a project I should complete with little opportunity to outsource elements.

Computing Resources. Computing facilities are plentiful on the University Brayford campus with 24/7 access.

Workshop Resources. The workshop is available for use on the University Riseholme campus, in conjunction with the engineering team and their availability.

Equipment. The primary equipment required is the hyperspectral camera which has been provided. Other aspects of the project are able to be built or purchased.

3.3.2 Time Management

Effective time management is important to realise the success of this project. In line with the constraints of the project, a plan was created to achieve the project's objectives.

Since this project demanded several elements to be brought together under reasonably tight deadlines, a waterfall approach to time management was decided. An agile approach would lend itself better to a project with fewer elements to integrate but had several iterations and to be worked on in a collaborative environment. Instead, the linear waterfall approach allowed this project to be planned from both ends, breaking the work into tasks, estimating the time and resources required and comparing this with the deadlines and time available and adjusting the scope of the project to create a deliverable plan.

3.3.3 Risk Management

Once a provisional plan had been created, it was important to understand the level of risk involved in whether the project may succeed or fail. The risk was managed by identifying potential hazards and rating the risk on a basis of severity and likelihood. The risk level was then evaluated according to the risk matrix given in Figure 3.2. Based on the risk level, it was decided whether further actions should be taken or the plan changed to reduce the risk of project failure. A red outcome means the risk level is high. A high level will not be tolerated as it puts the project's success in jeopardy and risk avoidance strategies must be employed to de-risk the hazard. Orange refers to a medium level risk. These risks can be accepted but it is desirable to reduce the risk to a low level using the same strategies. If the risk cannot be reduced, close monitoring shall be implemented and contingency must be planned such that fast and decisive action can be taken should the hazard occur. A green category refers to a low risk level. There is no requirement to reduce the risk but it can if easily done so. Contingency will not be planned for low level hazards because it costs to plan contingencies and given those hazards carry low risk, it is not worth planning for.

The approach to risk avoidance used four strategies: avoid, reduce, transfer or accept. In the *avoid* strategy the hazard will be eliminated altogether. Often this will come at a significant cost such as a significant redesign of the project but it is desirable to eliminate hazards and sometimes it is necessary especially if the risk is high. The *reduce* strategy means the hazard will still exist but its risk level will reduce through

		Severity (Rank)				
		Negligible (A)	Minimal (B)	Concerning (C)	Critical (D)	Catastrophic (E)
Likelihood (Rank)	Highly Improbable (1)	A1	B1	C1	D1	E1
	Improbable (2)	A2	B2	C2	D2	E2
	Occasional (3)	A3	B3	C3	D3	E3
	Probable (4)	A4	B4	C4	D4	E4
	Highly Probable (5)	A5	B5	C5	D5	E5

Figure 3.2: Risk matrix used for assessing risk level.

mitigating action. Mitigation may take the form of adjusting the solution design or it may take the form of finding out further information to become more certain in an assumption which may allow for the risk level to be derated. The *transfer* strategy aims to move the risk onto another party which often comes at a monetary cost. Examples include paying for insurance or outsourcing work to parties with expertise in that area. Finally, it may be decided to *accept* the risk. All risk must be weighed up with the cost of avoiding it, acknowledging that the time and resource used to combat a hazard is time and resource not being used to directly progress the project solution. In some situations, the best decision is to accept the risk.

Chapter 4

System Design

4.1 Understanding the System Context

An important first step before commencing the design of the system is to understand the needs that the system should fulfil and understand the context in which the system will operate. This will allow the system to be properly defined and requirements to be written.

During the initial meeting, the needs were established in discussion with the different stakeholders. A brief was formed to develop a system that could take pictures of crops using the Specim FX10 hyperspectral line scanning camera and develop a pipeline for processing the images. The imaging would be ground based and done on a scale of individual plants to obtain adequate resolution. The goal is that this system can be used to study disease in potato crops, in particular for early detection of blight, and ultimately in the field. The need for the right spectrum and intensity of light were discussed also.

A structural SysML diagram, shown in Figure 4.1 was created to understand how the system sits in context and the interactions. The connections headed with a black diamond are associations, and more specifically a composition. The diagram should be read that ‘the **Environment** is composed of a **Light Source**’, or alternatively, ‘the **Environment** “has a” **Light Source**’. This is a one-to-many relationship where only one **Environment** block is permitted but there can exist anywhere from one (1) to (...) many (*) **Light Source** blocks. The relationships between blocks are

indicated by rounded lines and should be read in the direction of the arrow such that ‘the Light Source illuminates the Plant’.

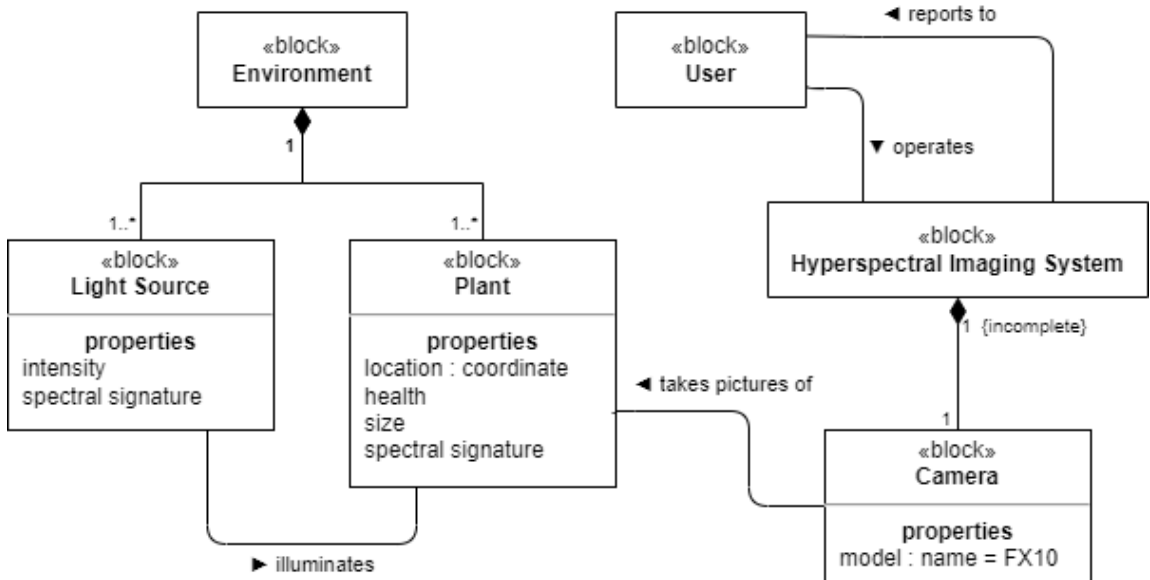


Figure 4.1: A structural SysML block definition diagram modelling the system context.

The diagram shows the hyperspectral imaging system to be developed has a camera whose model is the Specim FX10. This is an associative behaviour and is stipulated by the brief. The plants to be imaged are also shown as a block/entity. The plants exist in an environment and the association relationships shows there can be one to many plants in the environment. The plants have numerous properties such as their species, variety, location, size, and spectral signature. Only a selection of the most relevant properties have been included. As the background technical information research found, illumination is critical to hyperspectral imaging, both its spectral composition and its intensity. Consequently, the light has been modelled in this diagram. It is also understood that the properties of the light depend on the environment. For example, an indoor environment will have very different light to an outdoor one and even within each there can be much variability. Finally, it is very important to understand user and their role within the wider system context and as such it has been modelled. The user will operate the system and the system will report back to the user on status and results.

It was most important to make best progress toward the goal of a system capable of

in field automated hyperspectral imagery. As such the scope of the project had to be managed accordingly by designing an appropriate system.

Plant For the purpose of this project, the plants to be imaged were potato plants grown in individual pots in a poly tunnel on the University of Lincoln Riseholme campus. These will be grown as part of a study into the effects of different soil treatments, facilitating analysis of varying plant health. By being grown in individual pots this aids in easier system verification since the leaves of different plants will not be growing together.

Environment and Light Although the poly tunnel is not full field conditions, this is a sensible starting point. The plants will be under the effects of natural illumination, although not direct sunlight. The poly tunnels are much more accessible than a field, aiding rapid development by removing logistical challenges and the poly tunnels have mains electric should it be required.

User The expected users are academic researchers working on plant science or image and data analysis thus will have some level of technical skills but usability is still important. Ideally, the system should be operable by a single user. Ultimately a fully autonomous process is desirable to the extent a user isn't required, but for the purposes of this development a user shall operate any manual parts of the system.

4.2 System Decomposition

Considering the needs of the system and its environment, the problem was decomposed. The design is presented in Figure 4.2 as another structural SysML diagram and the design decisions are discussed herewith.

Firstly, the system was decomposed into two primary subsystems: Acquisition and Processing and a third component named Trolley. The Acquisition Subsystem is responsible for capturing the hyperspectral image of the crop and the Processing subsystem for performing corrections on the data and extracting insights. Apparatus is required to position the camera above the canopy and this didn't comfortably fit

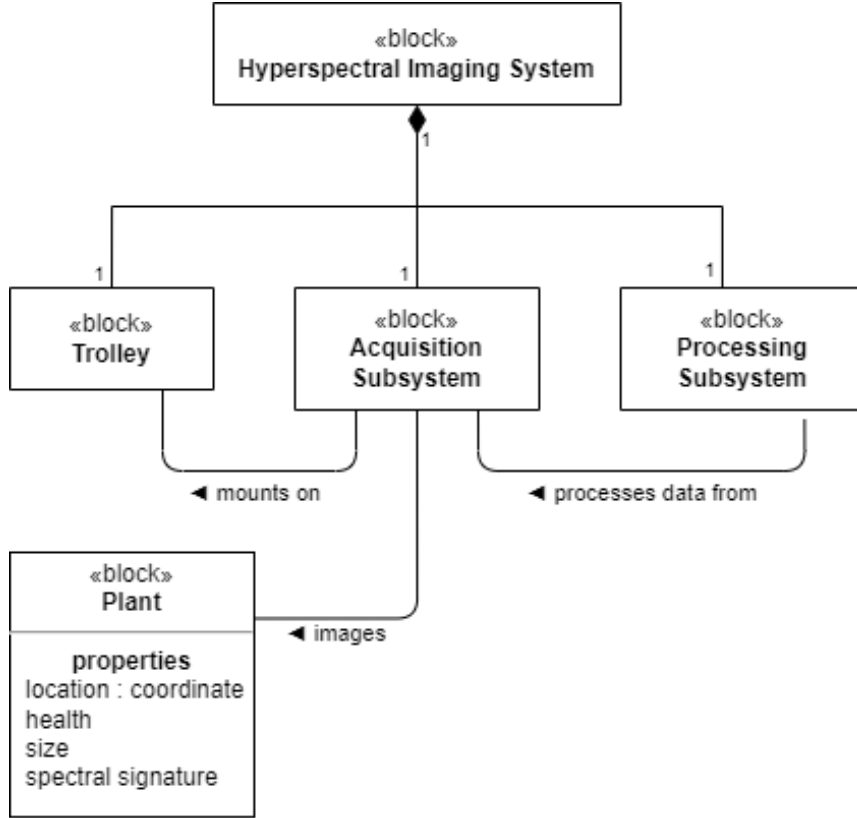


Figure 4.2: A structural SysML block definition diagram modelling the subsystem decomposition.

within the acquisition subsystem. Due to the uncertainty of the future uses of this system, it was decided to modularise the system such that the acquisition system is independent of the framework to suspend it. This means that the acquisition system can be attached to different forms of the trolley depending on the requirements of scanning a particular crop. That may be indoor or outdoor, canopy height, row width and the system may need varying levels of mobility or autonomy.

4.2.1 Acquisition

As stated, the FX10 camera will be used as the imaging device but that in itself puts a lot of requirements on this subsystem.

Firstly, the FX10 is a line scanning camera and as discussed in the literature review, that requires the camera move relative to the plant as the image is being captured. That gives two options, move the camera or move the plant. Many of the related works seen move the specimen, however, those systems tended to be used for small

samples, perhaps a single leaf cut from a plant. In this situation, it is more practicable to move the camera for several reasons:

- Pots of potatoes are heavy making them difficult to bring to the system and would require high power electronics to move.
- Moving the pot could make the stems and leaves move, introducing artefacts into the image.
- A system where the specimen is put on a moving platform would not translate to the field.

This necessitates hardware and control that will move the camera in a straight line over the plant canopy at a specific speed which is to be calibrated.

Secondly, the camera requires the plant to be illuminated by a source of sufficient intensity across the entire spectrum that is to be imaged. Consulting the research, it is learnt that the sun is a good broad spectrum emitter (perhaps the ideal) as is halogen lighting but LED or fluorescent lighting are not. Regarding the intensity, several sources say that HSI requires increased light intensity than conventional imaging modalities but a number (lux) has not been found. The illumination should also be as uniform as possible over the area to be imaged. Since the sun is so far away, there is high uniformity over a small area and volume. Contrast this to a point source that is very close, as the subject gets further from the source the intensity will decrease as the area increases, so lower leaves of the plant will be illuminated to a lesser extent. A further consideration is shadowing. On clear sky days its expected that natural lighting would pose challenges due to the direct sunlight casting shadows from the imaging apparatus and other leaves. However, on a slightly cloudy day natural illumination will offer a nice diffuse and scattered light offering even illumination and few sharp shadows.

Artificial illumination has benefits and drawbacks: a single source will create shadows but this could be overcome by using multiple sources, the lights can be positioned below the camera to avoid shadowing. If multiple sources are used, the effects of overlapping, edge artefacts, or dark spots should be considered to have uniform illu-

mination. The implementation should also be considered. Using natural illumination requires no work whereas using artificial illumination requires significant work. The lights must be mounted and most likely move with the camera, they must be electrically powered and they have significant power demands, especially since only 5-10% is converted to light output. Due to the fact that the sun is an ideal light source in many ways and the challenges involved in implementing artificial illumination the decision was to use natural illumination only. After all, a simple system is more desirable provided it does the job. It's anticipated there will be enough intensity due to the examples seen but some uncertainty remains. Performing captures in the polytunnel will de-risk this slightly by helping scatter the light and avoiding shadows and the system can be experimented with outdoors to test its limits.

4.2.2 Processing

The goal of the processing pipeline is to read the image captured by the acquisition system and analyse it to reveal insights about the plant that was imaged. The input end is quite well defined since it is determined by the output of the camera but yielding insights is an open ended goal. As such, this aspect will be worked on iteratively towards a goal.

This subsystem will first be required to read the image data which will be in the form of a hypercube. Next, in line with the research carried out, is to perform corrections on the image as to remove variances from the environment. This is important so that each image is presented to the analysis part of the pipeline uniformly. Expected variances are the illumination source intensity and spectral composition and there may be spatial variances too although many of these will try to be designed out in the acquisition subsystem.

Python was chosen as a suitable environment in which to implement this processing. MATLAB was also considered and has good inbuilt tools for viewing hyperspectral images but Python has wider support for data processing, is open source, and has several options for managing large amounts of data.

Regarding the insights, a simple approach might be using properties such as biomass

or leaf colour, obtained from the image layers. However, this does not fully harness the power of hyperspectral imagery. The research showed that commonly, pixels were extracted and their spectrum used in a machine learning problem, often using dimensionality reduction to improve performance and efficiency. Whilst this utilises the spectra and can be extracted from different pixels, there is more information contained within relationships between pixels spatially that is not represented only by using the spectra. One way of incorporating these is to use image features, standard or hand-crafted, and pass these as features to the machine learning problem. An alternative way would be to pass the image or leaf to be classified to a deep learning problem such as a convolutional neural network. These options will be considered during the iterative design and implementation process.

Given the goal is to monitor the health status of plants, the output of the machine learning pipeline must be considered. One option would be to provide a health score as a continuous numeric output either as an absolute value or relative to some expected health or gold standard. This would require a regression problem to produce a continuous output, and in turn, appropriate data would be required. This would entail ensuring there are plants exhibiting health scores across the entire range of values expected and a reliable way to calculate a score for the plants. This demands quite a lot of work and is venturing outside the area of expertise, posing risk to the project. In addition, creating a scoring system that would generalise across different varieties and species is a vast problem that is beyond the time and resource available to this project. Instead, a classification problem will be used where the efficacy of the system is demonstrated by classifying plants according to different treatments they have been exposed to and broader classification of their performance as average, above or below.

In part, this subsystem will be used to verify that the acquisition system collects adequate images. Though the interplay of the two systems should be noted. Poorer performance in acquisition will put more demands on the correction elements of the processing system. This subsystem will be verified by its ability to correct the images that are input and then its ability to distinguish and classify plants of different treatment. This will also be the validation of the system.

4.3 Feasibility

At this stage, it was useful to pause and consider the feasibility of this design, including the timeline and risks. The initial risk assessment is given in Table 4.1

Table 4.1: Initial risk assessment.

Hazard and Consequence	Risk	Decision	Risk
System design inadequate for needs (actuation). Redesign or unable to deliver.	B1	Accept: mature area and alternatives available.	
System design inadequate for needs (illumination). Redesign or unable to deliver.	C4	Avoid: illumination critical to other project aspects and significant uncertainty. Redesign project to include artificial illumination.	A2
System design inadequate for needs (processing). Redesign or unable to deliver.	B2	Accept: processing subsystem has no dependencies and is to be built exploratory. Several methods identified in literature.	
Failure to get camera working. Unable to collect data to test acquisition system and build pipeline.	D3	Avoid: poses a significant threat to the project so try the camera out.	B1
Plants to image fail. Unable to collect data to test system and build pipeline.	C3	Transfer: other people will grow and care for plants. Reduce: severity reduced by finding multiple plant sources. Accept: monitor plant growth regularly.	B1
Damage to system or equipment breakdown. Incur time delays or unable to finish project.	C2	Accept: no further action identified that will reduce risk. If it occurs contingency plan is to identify replacements as soon as possible or proceed with partial system completion.	
Loss of digital work and data. Incur time delays	B1	Accept: unlikely to occur due to backup procedures and work distributed across physical and intellectual.	
No or restricted access to facilities. Unable to build hardware.	B2	Accept: maintain communication with staff.	

Project requires more time to complete than available. Unable to deliver complete system and test.	B2	Accept: plan shows completion in time available with float, not catastrophic if partial project completed.	
Delays or inavailability of parts. Incur delays or prevent manufacture of system.	C4	Reduce: order from reputable UK based suppliers, allow for extra time and monitor delivery.	B2
Unforeseen project elements arise. Incur delays or unable to deliver system as specified if new elements are too challenging.	B2	Accept: risk already low due to decomposition with V-model and support found in literature.	

The risk assessment showed there was concern over the length of time required to get the camera and acquisition software working due to the technical uncertainty in the process and that there was uncertainty in over relying on natural illumination. If there were several cloudy days with reduced intensity there may not be enough light to get sufficient dynamic range, or perhaps not even enough light on a sunny day. At this stage, it is unknown how robust the system will be to what scale of variation in illumination and there is concern this could make the processing unviable whereas artificial illumination would be unvarying. Furthermore, there are aspirations to use this system as a flexible tool going forwards for both outdoor and indoor use where artificial illumination is a necessity.

These risks were too high to accept therefore mitigating action must be actioned. It was decided to do an initial component test to power up the camera and connect it to the computer to verify it worked and to ensure it would capture data. Secondly, it was decided to bring artificial illumination inside the scope of the task.

The tests took longer than expected but verified the camera was working and the acquisition laptop communicating to the camera and receiving data. Initial research into Specim Lumo software via their tutorials had shown it controlling the linear actuator by setting speed and stop and start points that were in sync with the camera. Communications with the company revealed these options were only available to scanner products purchased from the company. These exploratory tests greatly

reduced the uncertainty in this area and has helped identify how components will interact and the greater amount of work that will be required. The feasibility was reconsidered and the updated hazards shown in Table 4.2.

Table 4.2: Revised risk assessment.

Hazard and Consequence	Risk	Decision	Risk
System design inadequate for needs (illumination). Redesign or unable to deliver.	A2	Accept: including artificial illumination in scope so should always have light.	
Failure to get camera working. Unable to collect data to test acquisition system and build pipeline.	B1	Accept: initial tests succeeded in acquiring an image through the software.	
Project requires more time to complete than available. Unable to deliver complete system and test.	C5	Reduce: change of scope and initial exploration has introduced significantly more work; remove time series acquisition from scope. Accept: monitor medium risk and be prepared to limit pipeline development if hazard materialises.	B3

This identified there was a high risk of not completing the system in time for testing and the imposed deadline. With increased burdens on the build from the new illumination and custom control interface requirement, there was also not enough time to build the system to begin collecting images of plants from an early stage that allowed for time series data to be obtained and analysed. Removing the time series collection plan brings the risk down to medium from which point the risk will be accepted and monitored. Should time become short at the end, the contingency is to remove some of the processing tasks from the scope. This will limit the validation of the system but shouldn't impact its development significantly.

4.4 Final System Design

Considering the requirements of each subsystem, stated in the sections above, the structural decomposition as shown in Figure 4.3 was decided upon. The details of each component will be discussed in their respective section in the following chapter.

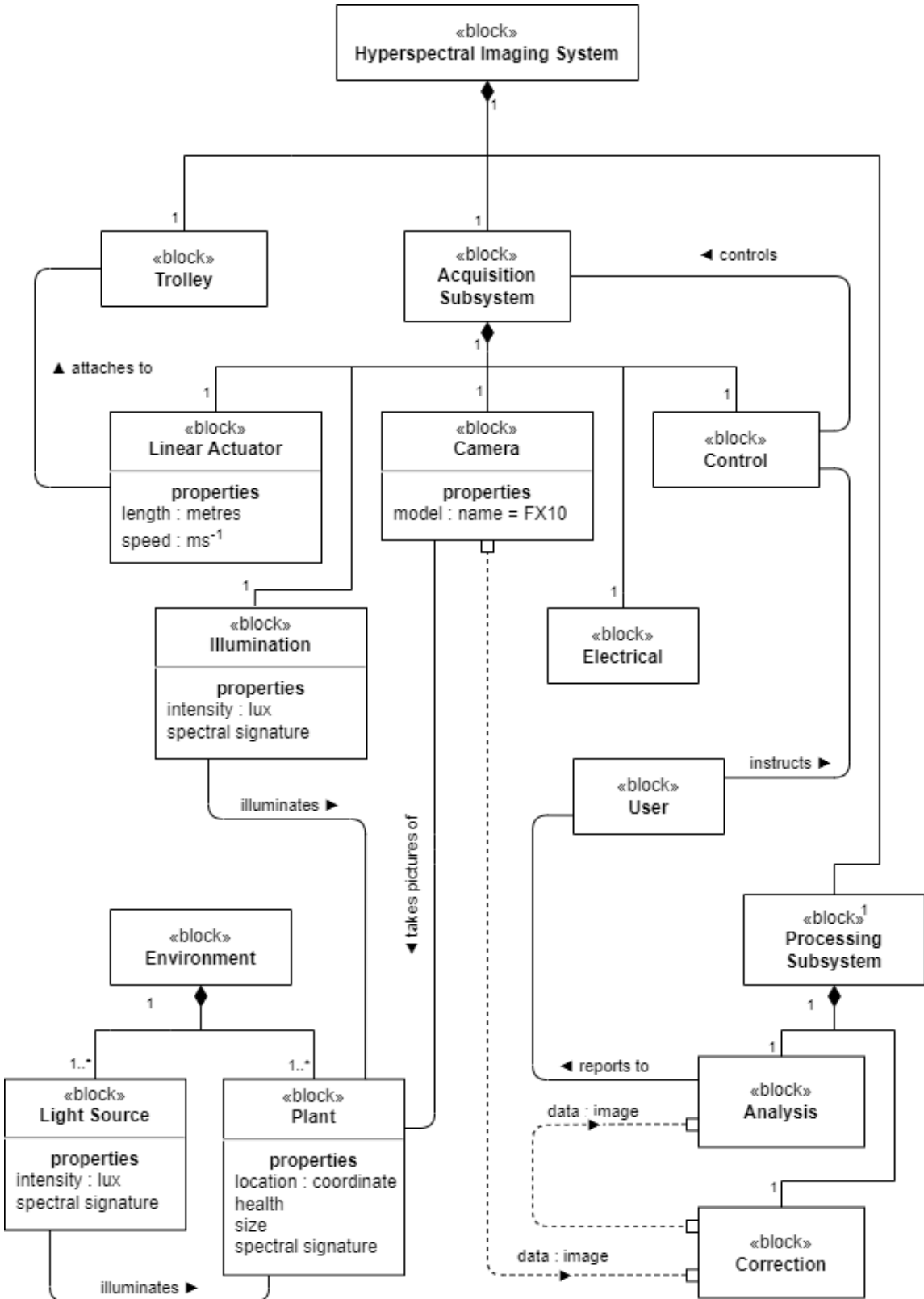


Figure 4.3: Structural SysML block definition diagram for the final system design.

Chapter 5

Development

5.1 Acquisition Subsystem Development

5.1.1 Camera

The camera to be used is a Specim FX10e and from its datasheet¹ some subsystem specifications were obtained. The spectral range is 400 - 1000 nm and it has 224 spectral bins and 1024 pixels along the length of the line. The camera has a 38° field of view (FOV) meaning the camera must be positioned approximately 500 mm above the canopy to get the plant in the frame. The weight of the camera is 1.4 kg and its dimensions 150 x 85 x 71 mm. The camera requires 12 V 4 W power supply and a GigE connection and at least 60 mm must be left behind the camera for these connections. Due to the system design, a white reference panel needs to be placed in the image across the entire line of pixels so that calibration can be done during processing.

5.1.2 Illumination

The requirements for the illumination system are as follows:

- The system shall illuminate the area to be imaged.
- The system shall provide broad spectrum light from wavelength 400 to 1000 nm which is inline with the wavelengths imaged by the camera.

¹<https://www.specim.fi/downloads/Specim-FX10-Technical-Datasheet-01.pdf>

- The system shall output 10000 lux at maximum output.
- The system shall illuminate the area uniformly.
- The system should avoid creating shadows that can be seen by the camera where avoidable.

As discussed in the previous chapter, halogen light is a good source of broad spectrum light and is affordable and readily available. A lot of energy is wasted as heat which is a concern, since both more energy will be required which is a limited resource with a battery powered system and that care must be taken not to damage or stress the plants by exposing them to too intense heat. However, it is critical to have broad spectrum emission thus these are costs that have to be paid.

One of the first considerations is how to position the lighting. Namely, whether it will be statically positioned and illuminate the whole area to be imaged or whether it will move with the camera to light up a more focused area where the camera sees. The former is a simpler solution in terms of the mechanical demands but lacks performance in other areas. For example, requiring 10000 lux over a large area will require significantly more light than if it were focused on a small area. This puts increased demands on the number of fittings required and their size as well as their power consumption. Since the lighting is halogen which already has a high power consumption per lumen output and the system is to be battery powered so consumption should be minimised, this presents challenges for a static system to cover the whole area. Further, if one light were used it would be challenging to light the entire area uniformly due to the spread and if multiple were used it would be challenging due to overlapping areas. Additionally, the mounting position must be considered not to collide with the moving camera and not to allow the camera to block any light. For these reasons, a lighting system that moved with the camera was chosen.

Three of the main types of lamp are capsule, reflector and linear and are illustrated in Figure 5.1. Capsule lamps are readily available at affordable prices and come in small form factors so would be easy to integrate physically. Their downside is without an external reflector, the light disperses in many directions meaning excess

light is wasted lighting areas that aren't required and can suffer from nonuniform illumination due to the shape of the glass. The linear lamp has the same drawback in that it comes without a reflector so much light is wasted, however, the light emitted from the linear lamp is highly uniform and since the requirement is to light a single line of pixels the linear style is very suited to this application. A reflector could be fitted, aiming to maintain uniform distribution though many off the shelf versions are most suited to flood applications rather than lighting a specific area. The reflector style lamp was chosen to be most appropriate since the reflector is integrated, directing the light towards a target, is available in different beam angles and offers reasonably uniform illumination. The reflector style lamp with a GU5.3 fitting is also Widely available for low voltage applications (Superior Lighting, 2022).



Figure 5.1: Types of halogen lamp. Images from Lightbulbs Direct, 2022

The next aspect to consider is how to configure the lamps to minimise the light wasted outside the area of the line of pixels and get uniform coverage in that area. The reflector lamps emit a cone of light, or if projected onto a planar surface, a circle. This inherently poses a problem for shining light into a thin rectangle about 400 mm by 50 mm (width chosen to add buffer). One approach would be to have an array of narrow beam lights, as illustrated in Figure 5.2.

A concern with this approach is the interfaces between the light from each lamp. There is a very fine line between overlap of the light causing a bright spot and a gap between them causing a dark spot. Even in the ideal situation, the two circles would not uniformly fill the entire 50 mm width and when real world inaccuracies enter it would be easy not to have uniformity.

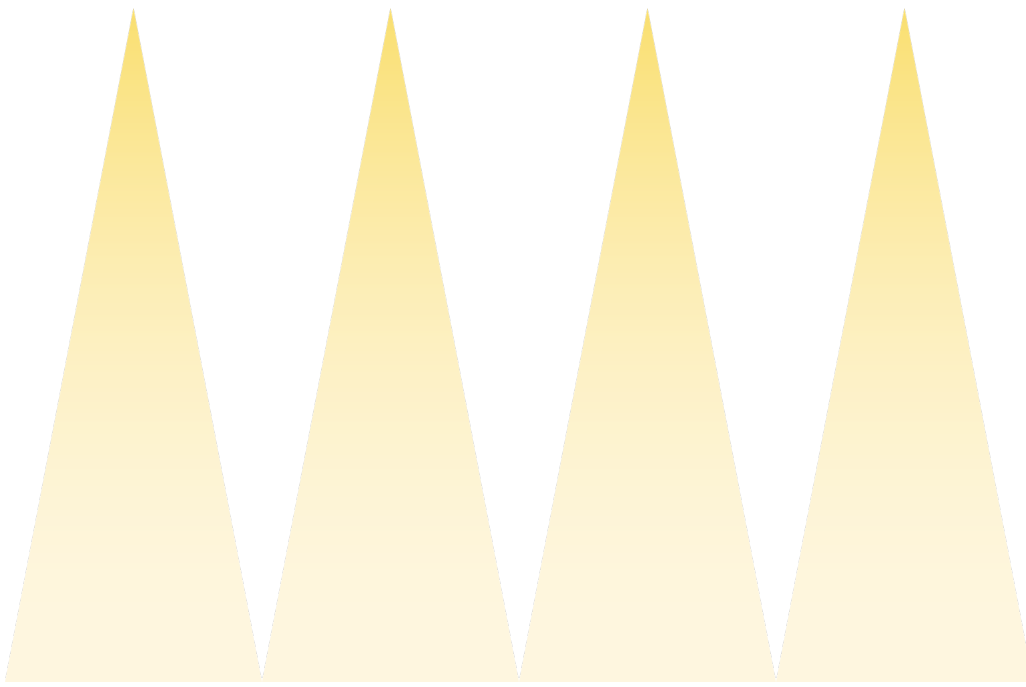


Figure 5.2: Example configuration of 4 narrow angle lamps in an array.

A way to avoid this is for a lamp to illuminate the entire area. If only a single lamp were used, shadowing would be caused that could be seen by the camera unless the lamp were in exactly the same place as the lens which isn't possible. To avoid this, it would be necessary to use multiple lamps to illuminate the entire area, in a setup such as shown in Figure 5.3.

As discussed in the paragraph before, the lighting needs to come from slightly different directions to avoid shadow, thus the arrays of light are mirrored on either side of the camera.

The biggest drawback to the above approach is the light wasted outside the area of interest, approximately 64% utilisation for the design in Figure 5.2 and 16% for the design in Figure 5.3. A solution considered was to use a plano convex cylindrical lens which would focus the light along one dimension. This would help to alleviate the problem but since the incident light would be of circular cross section, it would concentrate more light in the middle portion of the rectangular area of interest leading to non uniformity. For this reason and other factors such as the lenses being difficult to obtain and increasing the complexity of the project it was decided not to pursue this idea.



Figure 5.3: Example configuration of 2 wide angle lamps in an array.

The configuration and number of lamps has been chosen but now they must be positioned relative to the light. Since light intensity decreases with distance by a square relationship, if incident light is at an angle, the surface closest to the source will be brighter. Incident light at a shallow angle may help to illuminate more areas but it is only necessary to illuminate those that can be seen by the camera. For these reasons it is desirable to have the light as vertical as possible therefore as close to the camera lens as possible. Again, to ensure uniform illumination, it is desirable to have the lamps symmetrically placed. Due to the camera being longer in one dimension and the lens offset from the body, the lamps are placed to the side of the camera in the layout shown in Figure 5.4. The lamps are built with adjustability to allow them to be altered for targets that are closer or further away from the camera.

Due to the uncertainty in the level of illumination required, it has been decided to have the lights as dimmable. One option would be to control them electronically along with the motion hardware using a relay for on-off control or a power transistor. Instead, it was decided that manual control was sufficient for this project.

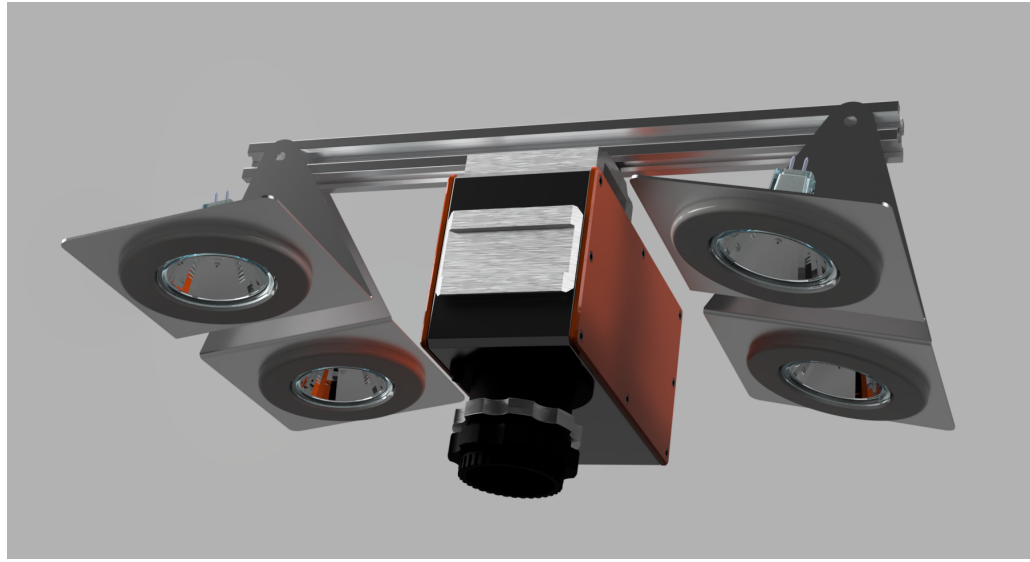


Figure 5.4: A render from the CAD model showing the lighting configuration and positioning.

5.1.3 Linear Actuator

The requirements of the linear actuator are as follows:

- The system shall securely suspend the camera and illumination system over the canopy.
- The system shall move the camera and illumination system perpendicularly to the line of pixels of the camera at a constant speed that is easily set by the user.
- The travel distance shall be 1 m.
- The motion shall be smooth.

First, several off the shelf solutions were considered. Specim sell several scanner solutions that integrate with the cameras and software, however, none of these met the requirements. Alternatively, linear actuators can be purchased as a single unit. It was decided not to pursue this option because they are very expensive, especially for long lengths, few met the speed requirements and there can often be constraints on controllability and challenges with integration rather than a custom built solution.

There are two aspects to the linear actuator, the carriage that supports the camera

and illumination system allowing it to move freely along one axis and the actuation of it.

Considering the actuation, the Pugh Matrix in Table 5.1 was used to decide on which drive type to use. Lead screw, belt drive and rack and pinion mechanisms were considered. They were scored against different criteria which were weighted according to their importance. The belt driven system had the best score.

Table 5.1: Pugh Matrix for selecting drive type.

Criteria	Weight	Lead Screw	Belt	Rack & Pinion
Cost	1	-	+	-
Ease of Implementation	1	0	+	-
Precision	0.5	+	0	0
Accuracy	0.5	+	0	+
Adaptability	0.5	0	+	0
Smoothness	0.5	+	0	-
Score		0.5	2.5	-2
Rank		2	1	3

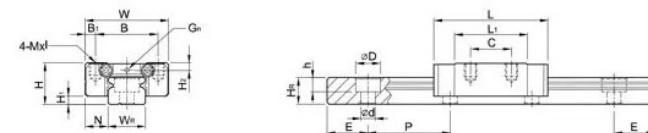
Next, the motor type must be chosen. A stepper motor was used for this application. The stepper motor will move a *step* which is a small but precise angle when commanded to. This can be done at high frequency, therefore the rate at which the motor *steps* determines the speed of the motor. Other motors such as DC motors have better torque and efficiency ratings but are more difficult to move at a specific speed. Furthermore, steppers are often used to drive timing belts therefore the hardware is available for the belt driven system. A kit using a stepper motor and belt driven linear actuator is available from Ooznest and their test data (Ooznest Limited, n.d.) shows a repeatability of 0.238 mm and accuracy of 0.260 mm which is adequate for this system. Parts will be sought to be obtained from this company.

Encoding is feedback so that the control system knows the position of the motor (or what it is moving). It was decided that encoding is not necessary for this problem. Stepper motors are mostly reliable at keeping their position and it does not matter if the camera does not return to exactly the right place, only that the scan motion is

correct. Furthermore, the user will be supervising the system and can get the system to reset if it loses its position. Since there is no encoding, the system will have to be initialised when it turns on since when the stepper motor loses power, the camera can move. For this, limit switches will be mounted at either end of the rail so a signal is sent to the control system when the carriage is at each end.

The last area to consider is the mechanism to provide the linearly constrained motion. The system presented by Ooznest in the paragraph above uses v-slot wheels that run on their aluminium extrusion. Another approach that is commonly seen is to use linear rails. These are linear bearings that attach to your moving carriage and glide along a precision machined rail which come in many profiles and specifications. These offer motion with very little play in constrained dimensions, very low resistance to motion and superior durability. Additionally they come with load ratings whereas the v-slot wheels do not. Due to the cables needing clearance at the back of the camera, the weight will be offset from the rail causing a cantilever moment to arise. Either two parallel rails can be used or a rail with a rated moment. The camera mass is 1.4 kg and an extra 1 kg allowed for other components. The centre of mass is assumed to be 50 mm from the centre of the rail. A force of 23 N and 1.15 Nm is required. Allowing for a factor of safety of at least 2. The specification of the MGN-12 rail (Figure 5.5) was found to be suitable.

MGN-C / MGN-H



型号	组件尺寸 (mm)										滑块尺寸 (mm)								导轨尺寸 (mm)				导轨的固定螺栓尺寸		基本额定负荷	基本静额定负荷	容许静力矩			重量	
	H	H ₁	N	W	B	B ₁	C	L ₁	L	G	G _n	Mxt	H ₂	W _r	H _r	D	h	d	P	E	(mm)	C(kN)	C _s (kN)	M _R	M _P	M _r	滑块	导轨			
																						N-m	N-m	N-m	kg	kg/m					
MGN 7C	8	1.5	5	17	12	2.5	8	13.5	22.5	-	Ø1.2	M2x2.5	1.5	7	4.8	4.2	2.3	2.4	15	5	M2x6	0.98	1.24	4.70	2.84	0.010	0.22				
MGN 7H							13	21.8	30.8													1.37	1.96	7.64	4.80	0.015					
MGN 9C	10	2	5.5	20	15	2.5	10	18.9	28.9	-	Ø1.4	M3x3	1.8	9	6.5	6	3.5	3.5	20	7.5	M3x8	1.86	2.55	11.76	7.35	0.016	0.38				
MGN 9H							16	29.9	39.9													2.55	4.02	19.60	18.62	0.026					
MGN 12C							15	21.7	34.7	-	Ø2	M3x3.5	2.5	12	8	6	4.5	3.5	25	10	M3x8	2.84	3.92	25.48	13.72	0.034	0.65				
MGN 12H	13	3	7.5	27	20	3.5	20	32.4	45.4	-												3.72	5.88	38.22	36.26	36.26	0.054				
MGN 15C	16	4	8.5	32	25	3.5	20	26.7	42.1	4.5	M3	M3x4	3	15	10	6	4.5	3.5	40	15	M3x10	4.61	5.59	45.08	21.56	0.059	1.06				
MGN 15H							25	43.4	58.8													6.37	9.11	73.50	57.82	57.82	0.092				

注 : 1 kgf = 9.81 N

Figure 5.5: Specification of MGN rail.

The design was modelled in fusion and iterated until the specifications had been suitably met and to keep making changes to refine the design as components were sourced. Figure 5.6 show an aspect of the CAD design and the whole model can be explored interactively at this link <https://a360.co/3S3eqhR>. Figure 5.7 is a photo of the implementation of the design of the linear actuator.

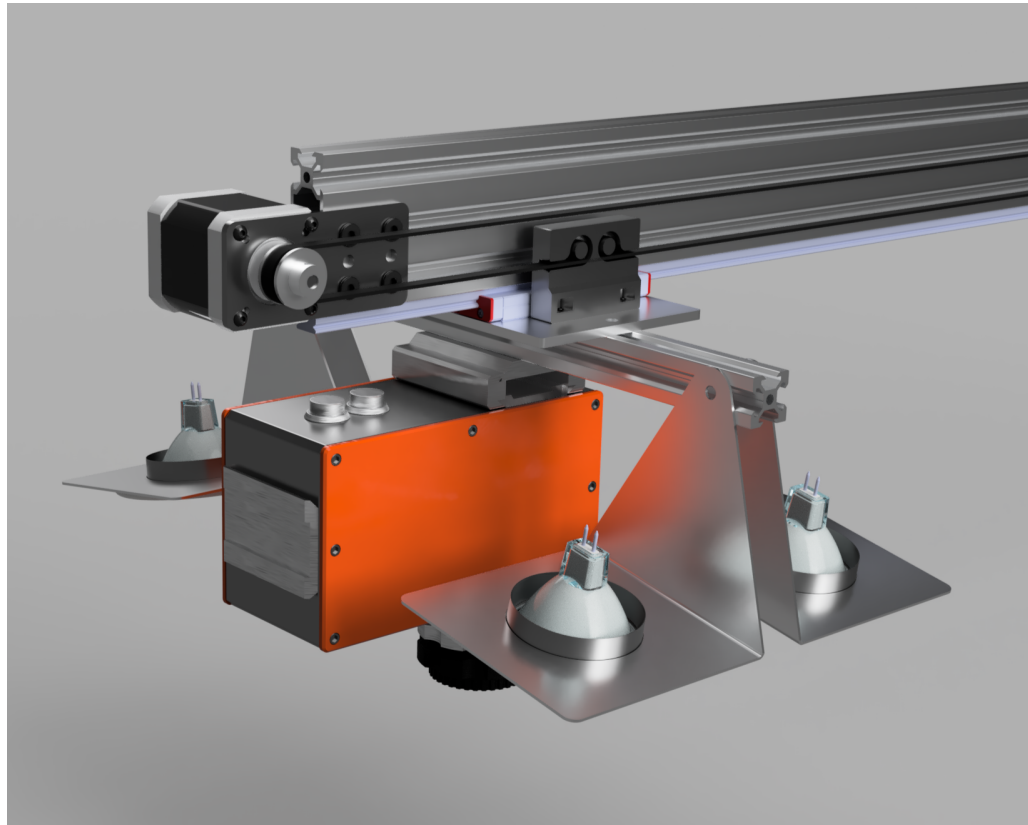


Figure 5.6: Fusion 360 CAD model of part of the linear actuator.

Several considerations were required to mount the rail, the motor, the belt and the carriage, lighting and drag chain all in a small efficient space. A few highlights include the drag chain to ensure the cables did not get caught up in the moving parts and keeping the belt on the opposite side to the camera and cabling for similar reasons. The rail was mounted on the bottom because it is stronger in this direction and the camera offset to the side to allow cable access. The lighting holders were built differently the manufacturing availability on the day.



Figure 5.7: The built version of the linear actuator.

5.1.4 Control

The user will interact with the control system to operate the acquisition system. The control system shall interface with the linear actuator to move the carriage at a set speed and record the data from the camera.

The feasibility of having one interface to control the two aspects was explored. Specim's software LUMO is capable of controlling a motor but after discussions with the company, it was found they would only let it be used for their own hardware and the API is not open. There was the option to either use or modify other software that is available since the camera used the GigE protocol but this was decided against. The LUMO software was already available and set up with the camera and it performs some of the calibration of the camera by default. Due the potential cost and time required to explore and setup a new software platform it was decided to use the LUMO Recorder software on a laptop and build a separate control system for the linear actuator.

To control the actuator, a microcontroller was chosen to be used, specifically the

ESP32. These are embedded devices with no operating system and perform a single task on boot making them reliable. They are low power and have limited processing but generally speaking very accessible IO making them ideal for tasks like this. The ESP32 is a particular board that can be used as an Arduino but is generally more capable than most Arduino boards, more affordable and additionally this has Wi-Fi and bluetooth capabilities. The Arduino has its own programming language but is built on top of C++ and code can be uploaded via a USB connection or otherwise.

There are several options for driving a stepper motor but it is generally accepted to use a dedicated stepper motor driver, especially for high current applications. For this project, the TMC2208 driver was selected. It is externally powered and receives instructions from the microcontroller via two pins. The DIR pin indicates the direction of motion and when the STEP pin is pulsed the motor moves a step. This driver has advantages over others such as the DRV8825 since it is a silent driver and employs various methods to change the way it energises the coil to ensure a smooth motion and avoid overheating. The control of these drivers can be further aided by using a code library. The AccelStepper library was chosen for this due to its wide support and the feature of having variable acceleration. The acceleration will allow a smooth start and stop for travel moves. A nice feature over other libraries is that the position is kept track by the library.

It was said earlier that limit switches are required. The specifics will be covered in the electrical section but they will be connected to a GPIO pin of the ESP32.

A means is required for the user to interact with the control of the linear actuator. One option is buttons and/or a knob to control the speed but a software solution was favoured over this due to the ability to rapidly change and prototype features and display information in a flexible format back to the user. It was also decided to utilise the wireless capabilities of the ESP32 for communication rather than needing to run more cables and be constrained to its location and control. This lent itself to using a webpage as an interface for the control. This had advantages of a command line or graphical user interface for both the developer and user. A web page is very versatile in the information it displays and does not require a specific application to

be installed on a specific device. The webpage is served by the ESP32 and it could be accessed from the laptop with the LUMO on or a mobile device if more flexibility is desired.

To implement the control system a sketch was written that reads the switch inputs, outputs to the motor driver and serves the webpage. The webpage files are stored in the ESP32 memory using the SPIFFS filesystem and uploader. The code that implements the control system can be found at <https://github.com/bennett-j/line-scan-actuator>

5.1.5 Electrical

It was decided to operate the system at 24 V since that reduced the current demand for the lighting so meant smaller cables and components could be used. The stepper motor driver would run on 12 V but it benefits from the higher voltage. The system is run off two 12 V batteries wired in series. The supply is fed to a fuse box from where circuits go to power the electronic control box on the actuator, the lighting circuit via the dimmer switch and to power the router via a 12 V step down converter.

This can be seen in Figure 5.8

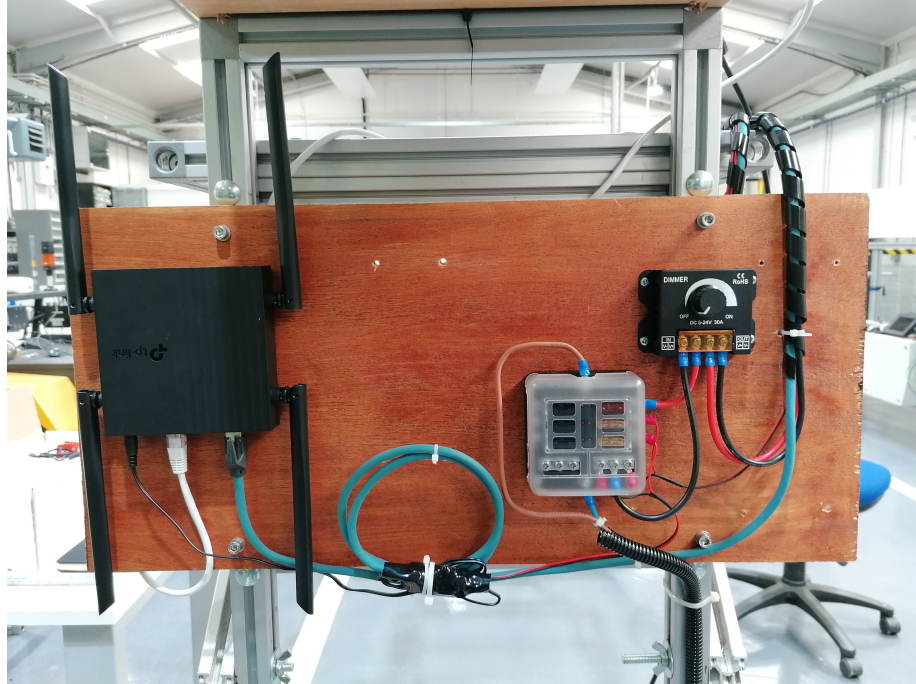


Figure 5.8: A photo of the main electrical system.

A photo of the electronic control board that was made for this project can be seen in Figure 5.9. The 24 V supply comes in at the top left which supply the two step down converters, the first at 12 V that exits bottom left for the camera supply and the other set to 5 V to supply the ESP32. The ESP32 is in the middle and has more connections underneath which receive the limit switches which are connected to the black and blue spiralled cable. It also connects to the stepper motor driver with the blue heat sink that picks up the 24 V rail for power and outputs to the motor on the right. The limit switches are set to input pull up pins and connected to ground. They are wired in the normally closed configuration to improve safety because if there was a fault and a cable broke the switches would appear depressed to the microcontroller which would stop the actuator.

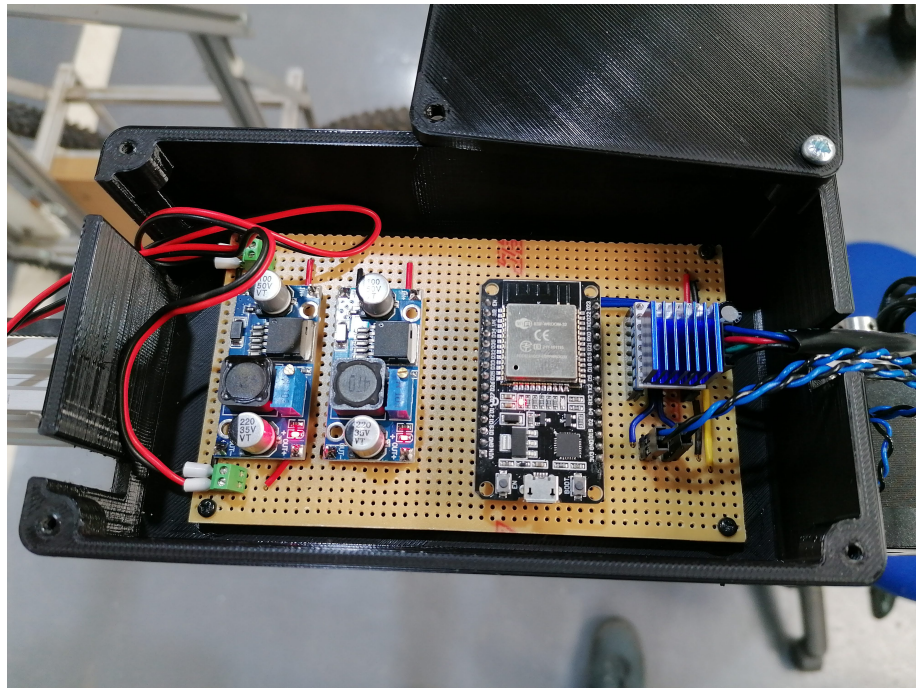


Figure 5.9: A photo of the circuit board built for controlling the actuator.

5.1.6 Cart

The cart was modified from an existing platform to be suitable for this application of the right height and width. The actuator and electrical system were attached to the cart. A frame was also built to suspend the white reference panel below the camera

at the start of the imaging so that it was always in frame and always in the right place.

5.2 Processing Subsystem Development

Since the processing subsystem was built in an iterative agile way without fully specifying the system, this report will follow a similar pattern discussing the design, implementation and testing in parallel. The processing subsystem is comprised of two main parts: correction and analysis. The data is passed from the acquisition system to the correction and then to the analysis.

5.2.1 Correction

The goal of the correction system is to remove variances in the image that are a result of variations in environmental factors and remove artefacts arising as a result of the imaging process. Since this inherently requires an understanding of how good the images captured were, this will form part of the verification for the acquisition sub system.

First the image must be read into python for which the library Spectral Python was used. The images are saved in the ENVI file format from the software and the folder contains a header file which points to where the data is and a number of properties of the image. This file is given as an argument to the function `open_image()` which returns an object able to access and read the data which is not immediately loaded into memory due to the data size of several hundred megabytes.

A sample image was selected for the purpose of this report with no artificial illumination which is a capture of a potato plant grown in a pot in a polytunnel. It is inherently difficult to show three dimensional data simultaneously so these RGB images have been created by extracting certain wavelengths; the raw image is shown in Figure 5.10. The line of pixels is in the x direction and the scan direction was the y direction positive. At the top of the image the white reference panel can be seen before the plant is captured. The data has been scaled to fit in the range [0 1]

... but as can be seen, the panel does not appear white and, by inspection, several of the values are in the range [0.75 0.85]. This is in part an artefact of the bands that were selected but also due to noise in the image and variation in the incoming illumination. These are all aspects that must be addressed in the correction phase.

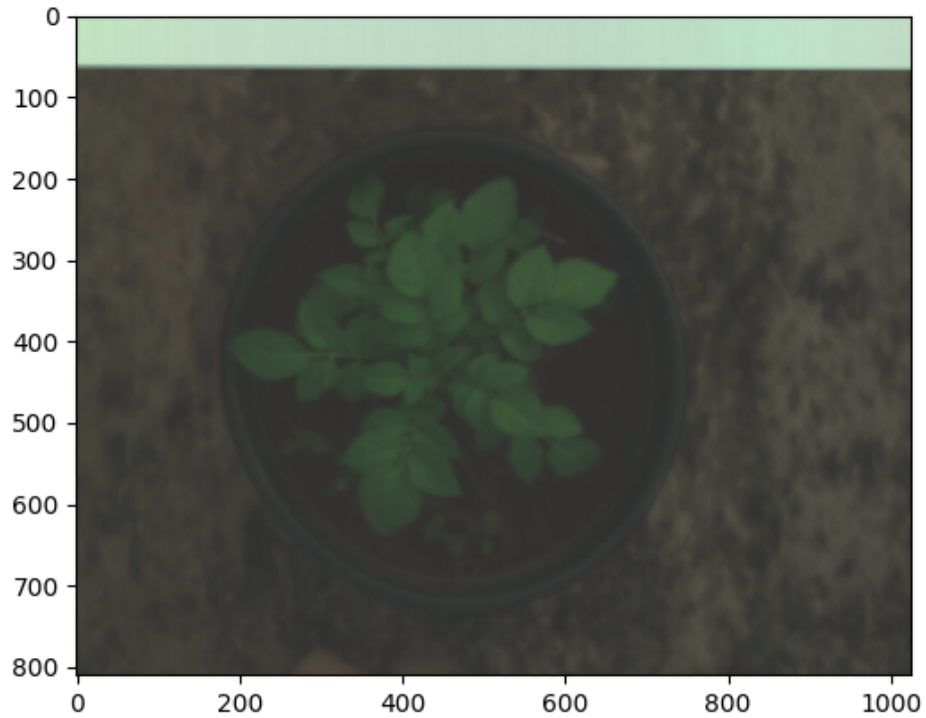


Figure 5.10: Raw image of sample plant using R = 650 nm, G = 530 nm and B = 466 nm.

To illustrate the spectral dimension of the data, the spectra for individual pixels has been plotted in Figure 5.11. Considering first the spectral response for the white reference panel, the panel should reflect over 99% of all incoming radiation therefore it is good to see the intensity is greater than all other pixels at all wavelengths and this spectral signature should be close to that of the incoming radiation. However, it is worth noting that this radiation is not uniform across the entire spectrum, thus it is more convenient to deal with percentage reflectance. It is also worth observing that the white reference panel, leaf, and background areas have noticeably different spectral compositions.

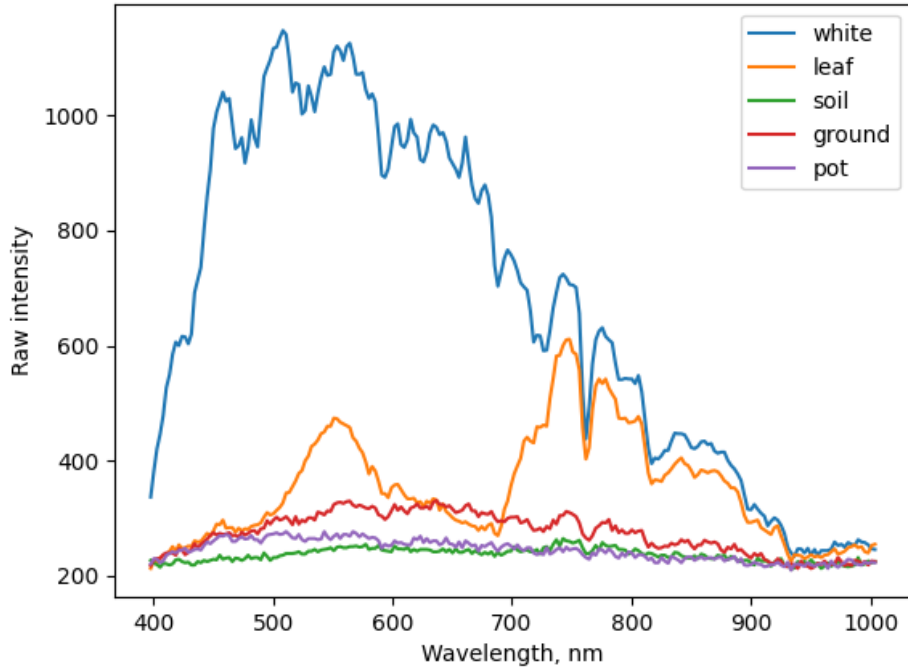


Figure 5.11: Spectral signatures of pixels from different parts of the image in Figure 5.10.

Figure 5.12 illustrates differences in incoming illumination from indoor and outdoor environments with and without artificial illumination. This is evidence that in different environments the intensity and spectral composition of the incoming radiation vary. Without correction, the different illumination would result in different spectral signatures of the plant pixels. To compare the similarities of the spectrum (disregarding average intensity), one spectrum, L , was divided by another as per Equation 5.1 then it was zero centred by subtracting the mean and the sum of squared errors calculated as per Equation 5.2, yielding a scale invariant similarity.

$$R = \frac{L_A}{L_B} \quad (5.1)$$

$$\epsilon = \sum_i^n (R_i - \bar{R})^2 \quad (5.2)$$

The results, given in Table 5.2 show that the polytunnel versus outdoors with the same artificial illumination have a low error score indicating the spectra are similar.

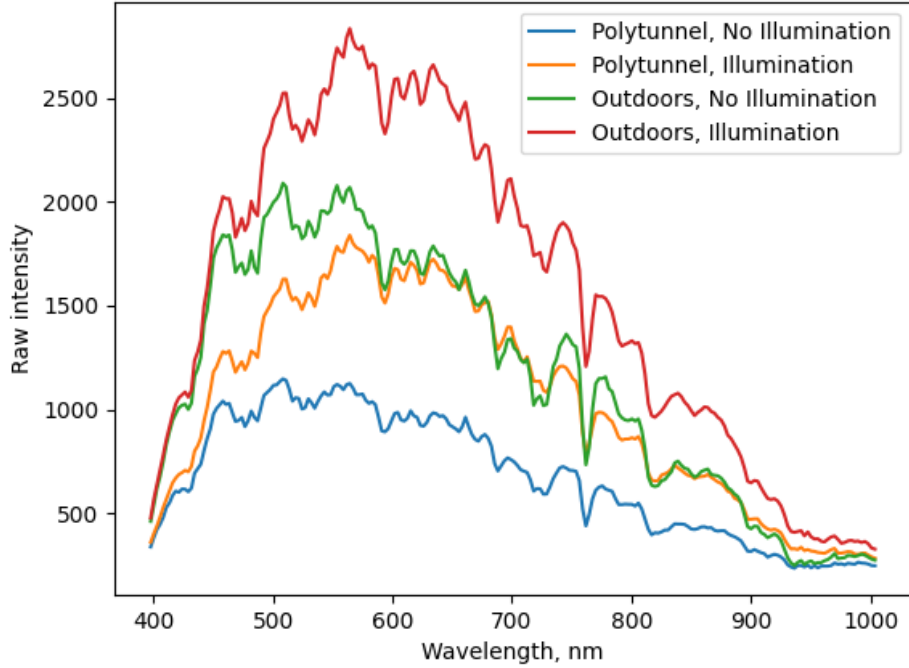


Figure 5.12: Spectral signatures of pixels from the white reference panel under different illumination environments.

It is good to know that the polytunnel is not filtering out any wavelengths considerably but the intensity is reduced. In comparison, the similarity between with and without illumination shows a higher error score of 13.92 indicating that the artificial illumination does have an effects on the composition of the spectra. This was to be expected and can be addressed using the reflectance retrieval procedure.

Table 5.2: Table giving scale invariant similarity error scores as per Equation 5.2 for different illumination variations.

Environment & Lighting	Error, ϵ
Outdoor none : Polytunnel none	2.03
Outdoor full : Polytunnel full	0.33
Outdoor full : Polytunnel none	13.92

Something else to note is the maximal pixel value in the whole image is 1215 (close to the peak white value in Figure 5.11). The camera images in 12-bit values meaning the maximal intensity is 4096 therefore, in this image only 30% of the intensity range which affects the dynamic range of the image. The exposure time of the camera was

set close to its maximum which suggests since the sensor is far from saturation, more incident light would have improved the dynamic range. Consulting Figure 5.12, adding illumination in the polytunnel brings the peak value to approximately 1800, outdoors with no illumination to 2100, and outdoors with illumination to 2400. The artificial illuminations system still increased the intensity level by a noticeable amount when outdoors which was not anticipated. Despite these increases in intensity, only about 60% of the available dynamic range is still being utilised so there is scope to increase the light output of the artificial illumination system.

The next stage is to perform reflectance retrieval according to the formula given in Equation 2.2 from the literature. This formula uses the raw image and the dark reference to remove some effects of sensor noise and the white reference to calibrate for reflectance. The dark reference was captured and saved in another file and the white reference is extracted from the start of every image. Both references are two dimensional arrays across the image width and spectral dimension. The mean is averaged over the scan direction but reflectance must be retrieved over all wavelengths and differences in each spatial pixel corrected for. The formula is implemented by the code snippet illustrated in Listing 1

The results are visualised in Figures 5.13 and 5.14. The RGB image looks much clearer as if the colours have been enhanced and looking at the spectra it is seen how everything is set relative to the white reference panel. The noise especially at the higher wavelengths above 900 nm should be noted due to the low signal in the raw image. These will be removed for processing in line with the recommendations of the literature.

The literature advises to perform spectral smoothing on the images since it says consecutive wavelengths should be similar intensity. As noise can be seen in the spectra of Figure 5.14, it is appropriate to apply this smoothing. Paulus and Mahlein, 2020 advises to use a Savitzky-Golay filter with a window size of 15 and order of 3 for the Specim FX10 camera. Figure 5.15 shows the results of the smoothing and exclusion of the extreme bands.

To verify that the correction pipeline works, the corrected spectra of pixels extracted

```

1  from pathlib import Path
2  from spectral import *
3  import numpy as np
4
5  # Create file paths
6  scanName = 'PT_C_plant01_0046'
7  imgPath = capturesPath / scanName / 'capture' / (scanName + '.hdr')
8  darkPath = capturesPath / scanName / 'capture' / ('DARKREF_' + scanName + '.hdr')
9
10 # Read images
11 # If the file being opened is an ENVI file, the file argument should be the name
12 # of the header file.
13 im_proc = open_image(imgPath)
14 im_dark = open_image(darkPath)
15
16 # Average dark and white patches along scan dimension
17 mean_dark = np.mean(im_dark.load(), axis=0)
18 mean_white = np.mean(im_proc[0:50,:,:], axis=0)
19
20 # Perform reflectance retrieval
21 # Subtraction and division dimensions verified (https://numpy.org/doc/stable/use\_r/basics.broadcasting.html)
22 im_proc = (im_proc.load() - mean_dark) / (mean_white - mean_dark)
23 # Clip image for the few pixels that fall outside range [0 1]
24 im_proc = np.clip(im_proc, a_min=0, a_max=1)
25

```

Listing 1: Code snippet of reflectance retrieval

from images under different illumination were compared. It is known that the incoming illumination has a different spectral composition from Figure 5.12. A pixel was extracted from a leaf of the calibrated image shown in Figure 5.13 and one from an image of the same plant with the artificial illumination system on full. The image was calibrated using the pipeline and a pixel extracted from the same part of the same leaf. If the system is working optimally and the same part of the leaf chosen the two spectral signatures should be identical. The result is displayed in Figure 5.16.

Whilst the results (Figure 5.16) show similarity between the two leaf pixels, they are not identical. The two spectra have a similar shape but the illuminated one has greater intensity across the spectrum and is a near scaled version. On considera-

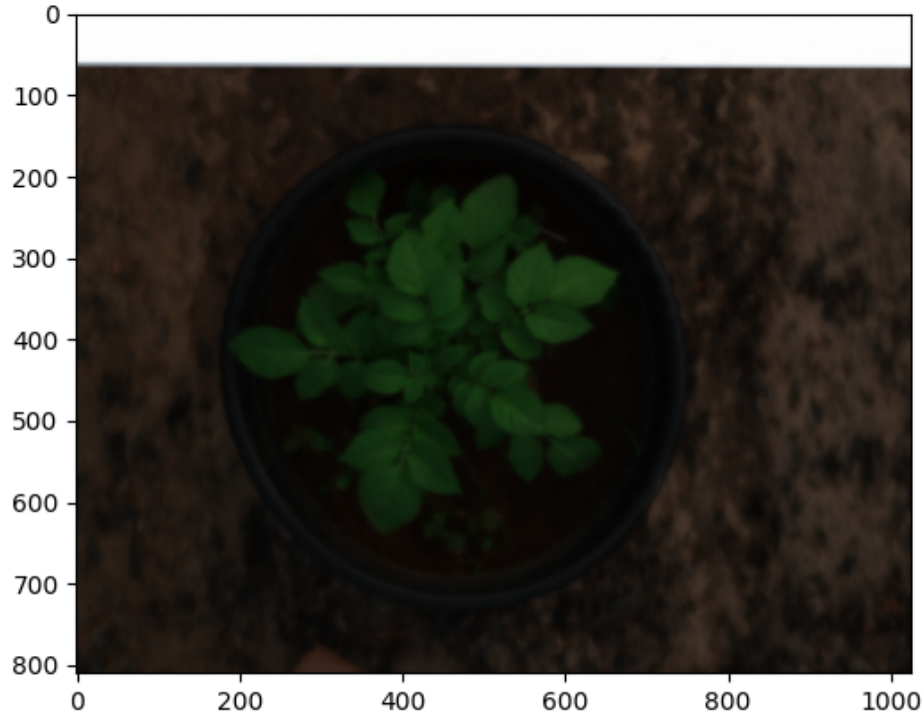


Figure 5.13: Reflectance calibrated image of sample plant using R = 650 nm, G = 530 nm and B = 466 nm.

tion, the presumed reason for this behaviour is because the the calibration panel is approximately 150 mm above the canopy of the plants. The explanation is that, as explained earlier in this report, as the target gets further away from the lamps, the light spreads out over a greater area and the intensity decreases. This means that the white reference panel would have been exposed to a greater intensity than the plant. When the image was corrected to make all whites the same intensity (reflectance of 1.0) this meant the plant was made darker to compensate, hence the effect seen in Figure 5.16. It is expected that these spectra would pose some challenges for the classification but that there would be an approach able to fit a model. For the rest of this processing, the artificial illumination will not be mixed. Optimally, this effect would be designed out of the system either by ensuring the white reference panel was always at the height of the plant canopy, or by ensuring the illumination doesn't vary with depth such as by parallelising the incoming light rays. If the effect can't be designed out, it's possible it could be corrected for if the distance to the panel and

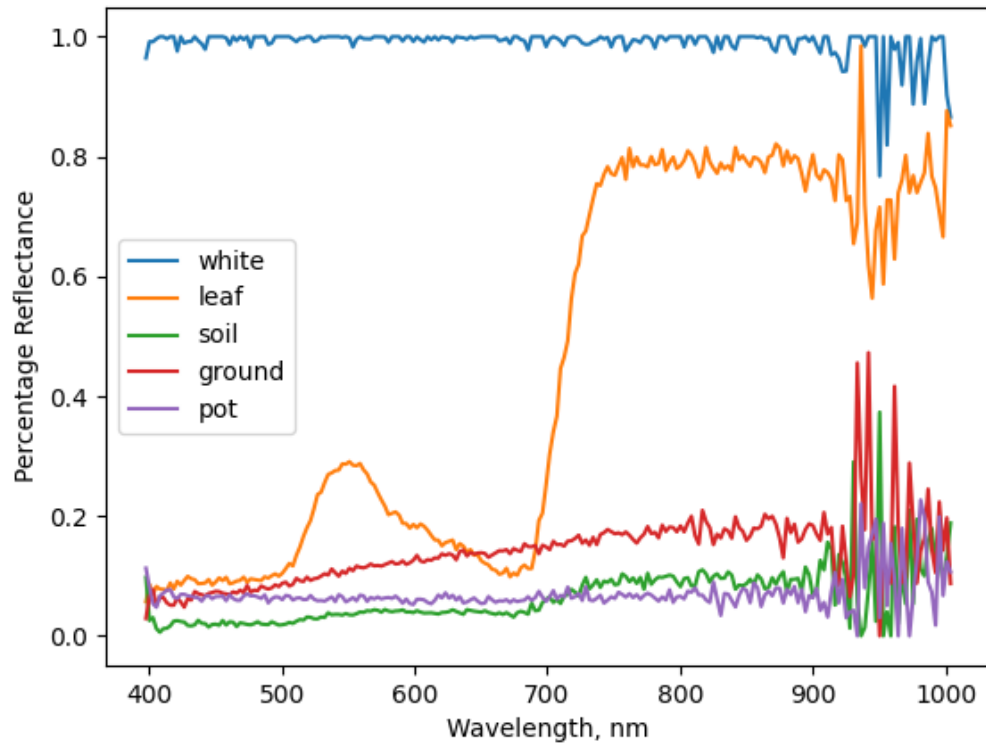


Figure 5.14: Spectral signatures of pixels from different parts of the image in Figure 5.13.

plant were known, for example with a sensor, knowing intensity, I , decreases with distance, d , from a point source with an inverse square relationship as per Equation 5.3.

$$I \propto \frac{1}{d^2} \quad (5.3)$$

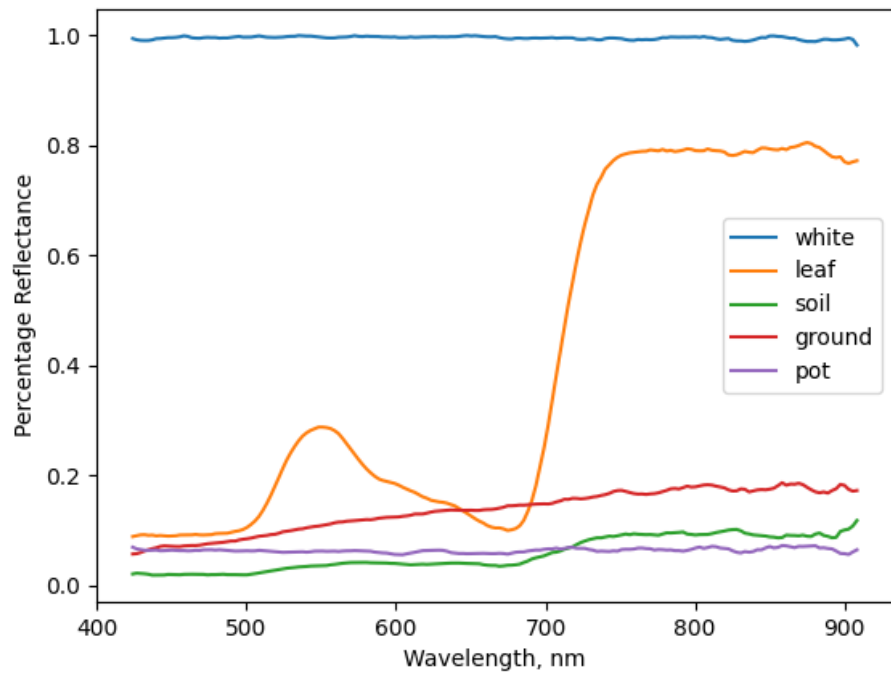


Figure 5.15: Spectral signatures of pixels from different parts of the image in Figure 5.13.

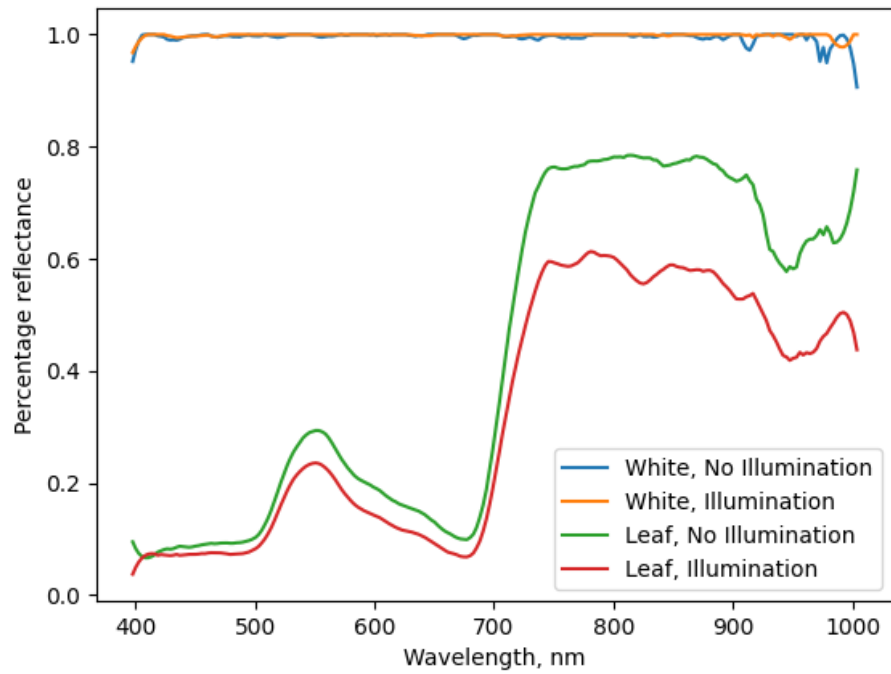


Figure 5.16: Spectral signatures of pixels from calibrated images of plants under different illumination.

5.2.2 Pre-processing

Now that the image had been corrected, the next stage was to prepare the image for analysis. Firstly, the regions of interest, being the plant, must be found and segmented from the image. Several approaches were explored and the Ratio Vegetation Index (RVI), as given in Equation 5.4, is the ratio of the Near Infra-Red (NIR) band to the red band. Vegetation typically has high intensity in NIR but low in red such that the RVI will be high for pixels with vegetation and this approach was found to work well. The RVI was applied to the image, yielding Figure 5.17 which is a grayscale image which was thresholded, with the threshold being determined by Otsu's method so that it is done automatically. The thresholded image was then eroded to remove the boundary pixels with the result in Figure 5.18. The code snippet for these steps is found in Listing 2.

```
1  from skimage.filters import threshold_otsu
2  import numpy as np
3  import cv2
4
5  # Vegetation index
6  #  $RVI = NIR / RED$ 
7  RVI = im_filt[:, :, 150]/im_filt[:, :, 95]
8
9  # Determine threshold with Otsu's method
10 thresh = threshold_otsu(RVI)
11 mask = RVI > thresh
12
13 # Erode once with 5x5 kernel
14 kernel = np.ones((5,5), np.uint8)
15 erosion = cv2.erode(np.float32(mask), kernel, iterations=1)
```

Listing 2: Code snippet of leaf extraction.

$$RVI = \frac{I_{NIR}}{I_{Red}} \quad (5.4)$$

The next aspect of pre-processing is dimensionality reduction. After excluding the first and last bands that had high signal to noise ratio, there were 180 bands left. This is a lot of features to pass to a machine learning problem and we know from earlier

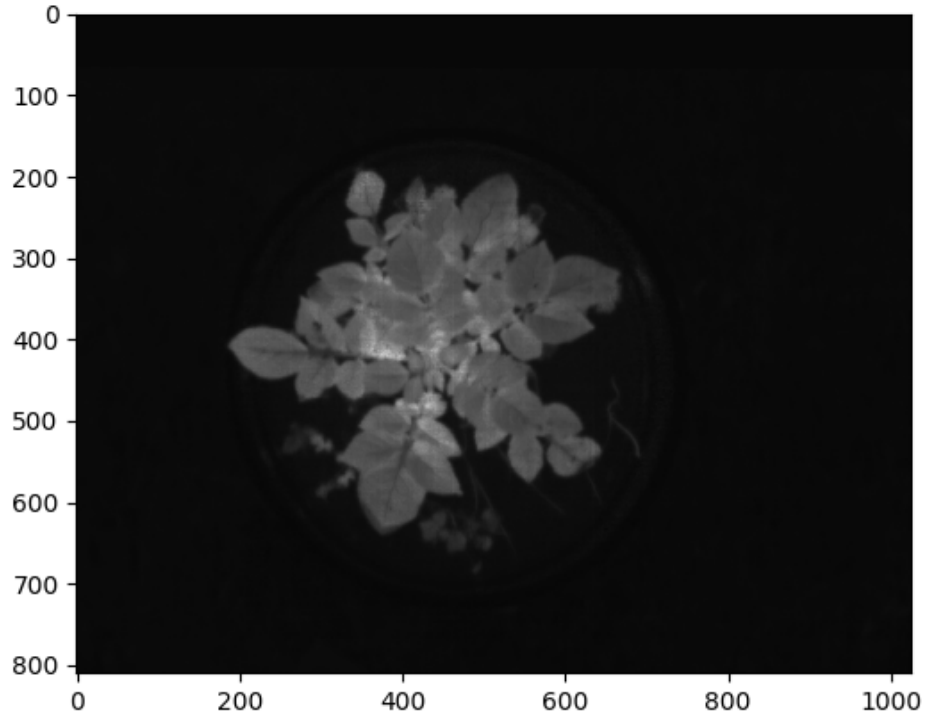


Figure 5.17: Image of the Ratio Vegetation Index applied.

assumptions that there are correlations with smooth changes between consecutive bands. Consequently there is a lot of redundant information in the data leading to inefficiencies in machine learning and potentially a decrease in performance. The method employed in this work is Principal Component Analysis (PCA) which is popular in many fields and recommended by many of the works surveyed in the literature review. PCA works by making new features which are extracted from linear combinations of the existing features. These are found through computing the correlation matrix and doing eigenvalue analysis on it, selecting those with the largest variance and extracting the new features. An alternative would be feature selection that finds the subset of bands that contain the most information and are most distinct from each other. These features are used unmodified and the others discarded rather than creating new features as combinations of existing features as in PCA.

The principal component analysis is done on one image and the transform that

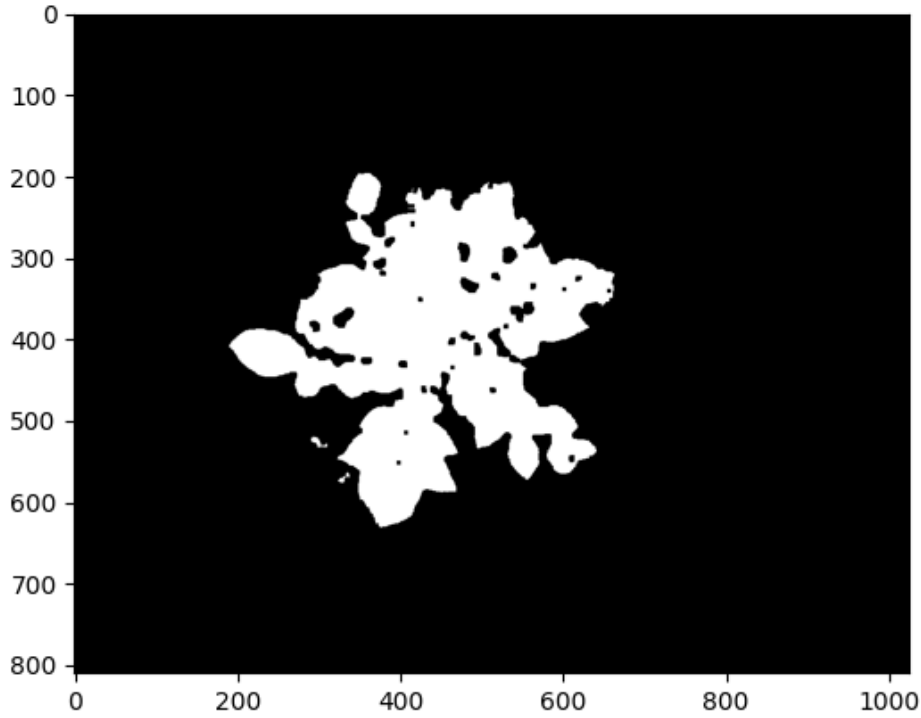


Figure 5.18: Image after thresholding and erosion.

extracts the top principal components is saved such that it can be applied to all the other images so that the same features are used for comparison. Experimentally, it was chosen to use seven features.

5.2.3 Analysis

Here, machine learning is employed to gain insights into the data. It was decided that the goal, in the first instance, is to classify individual pixels according to their spectral features. A set of features had already been extracted then pixels were sampled randomly from the leaf mask. This was split into a train and test set at 20%.

For this application, a supervised classifier is required where labelled data is passed to the algorithm to learn how to match the data to a label. The Gaussian maximum likelihood classifier was trialled due to its use in remote sensing of crops and its easy implementation via the Spectral Python library. The classifier learns how the data

of each feature is distributed by using its mean and standard deviation and makes predictions by evaluating these. This classifier failed to fit to the data and was not used. Further reading suggested its use was quite prevalent in remote sensing applications but not in close range imaging. Its expected this method would work well for classifying more distinctly different parts of the image such as crop type, bare soil, water as in remote sensing but is not suitable for our application.

Upon further exploration, and with the support of literature, the Support Vector Machine (SVM) classifier was deemed to be suitable for this application. The classifier transforms the data into higher dimensions and creates decision boundaries between the learned classes in that high dimensional space, aiming to find the hyperplane that maximises the margin to each class. SVM works in high dimensional feature spaces and is suitable for multi-class problems by breaking the problem down into multiple one-vs-one cases.

SVM uses kernels to transform the input data into higher dimensions and different kernels can be employed. Popular functions include linear, radial basis function, sigmoid and polynomial. These were tested alongside the tuning parameters in randomised search of the parameter space and the radial basis function (RBF) was found to perform best.

The SVM classifier has two tuning parameters, C and γ for the RBF. C is the regularisation parameter which considers the trade off between correctly classifying training data and maximising the margin. A high value of C will fit more closely to the training data but might lead to overfitting and generalise poorly. The value of γ affects the radius of influence of an individual training example and will influence the curvature of the decision boundary. A large γ results in a small radius of influence likely leading to overfitting but a small value will fail to capture the complexity of the data. The parameters were initially found using a random search alongside the kernel as above and then a grid search was used in the vicinity of the best values to further refine the parameters.

The scikit-learn library was used to implement the SVM classifier in Python. The complete pipeline is presented in Listing 3. The details of the scanned images are

saved in a CSV file which is read into python and saved as a dictionary, performing data conversions as necessary. Next, the images to proceed to processing are selected. Any images voided are not used and then the desired illumination settings and plant labels are specified. The selected images enter the pipeline to be read, corrected and pre-processed. Finally the classifier is trained.

Listing 3: Complete processing pipeline

```

1  from pathlib import Path
2  from spectral import *
3  import numpy as np
4  from scipy.signal import savgol_filter
5  import cv2
6  import csv
7  from enum import Enum
8  import random
9  from warnings import warn
10 from sklearn import svm
11 from sklearn.model_selection import train_test_split
12 from skimage.filters import threshold_otsu
13
14 # PREPARE FILES AND DETAILS
15 # use enums to define classes
16 class Labels(Enum):
17     TDYM = 0
18     TDNM = 1
19     BFYM = 2
20     BFNM = 3
21     NFYM = 4
22     NFNM = 5
23     NF = 6
24     BF = 7
25     TD = 8
26
27 # define file paths
28 captures_path = Path('/home/computing/Documents/james/captures')
29 details_file = captures_path / 'details_PT_C.csv'
30
31 # read details file and load as a list of dictionaries
32 details = []
33 with open(details_file, newline='') as csvfile:
34     reader = csv.DictReader(csvfile)
35     for row in reader:
36         if row["label"] != "None":
37             d = {'plantID': int(row["plantID"]),

```

```

38         'name': row['name'],
39         'void': False if row['void'] == "FALSE" else True,
40         'light': int(row['light']),
41         'class': Labels[row['class']]}

42
43     details.append(d)

44
45 # choose what scan parameters are to be selected
46 light = {100}
47 labels = {
48     Labels.NFNM,
49     Labels.NFYM,
50     Labels.BFNM,
51     Labels.BFYM,
52     #Labels.TDNM,
53     #Labels.TDYM
54 }
55
56 # define mapping to remap classes
57 label_mapping = {
58     Labels.NFNM: Labels.NF,
59     Labels.NFYM: Labels.NF,
60     Labels.BFNM: Labels.BF,
61     Labels.BFYM: Labels.BF,
62     Labels.TDNM: Labels.TD,
63     Labels.TDYM: Labels.TD
64 }
65
66 # extract chosen images from list
67 process_list = []
68 for entry in details:
69     if entry['void'] != True and \
70         entry['light'] in light and \
71         entry['class'] in labels: #and entry['plantID'] <= 5
72
73     # remap class
74     entry['class'] = label_mapping[entry['class']]

75
76     process_list.append(entry)

77
78 n_imgs = len((process_list))
79 print("Number of images selected: ", n_imgs)
80
81 # PIPELINE
82 n_features = 7
83 n_px = 5000

```

```

84 test_ratio = 0.2
85 n_samples = n_imgs * n_px
86
87 X = np.empty((n_samples, n_features))
88 y = np.empty((n_samples))
89
90 # set pc = None so we calc pc on first iteration then apply to all images
91 pc = None
92
93 # use a known number for some continuity during development
94 random.seed(0)
95
96 for i, scan in enumerate(process_list):
97     name = scan['name']
98     imgPath = captures_path / name / 'capture' / (name + '.hdr')
99     darkPath = captures_path / name / 'capture' / ('DARKREF_' + name + '.hdr')
100
101     # If the file being opened is an ENVI file, use name of the header file.
102     im_proc = open_image(imgPath)
103     im_dark = open_image(darkPath)
104
105     # REFLECTANCE RETRIEVAL
106     mean_dark = np.mean(im_dark.load(), axis=0)
107     mean_white = np.mean(im_proc[0:50,:,:], axis=0)
108
109     # subtraction below works because trailing dimensions have same dimension
110     # https://numpy.org/doc/stable/user/basics.broadcasting.html
111     # element-wise division
112     im_proc = (im_proc.load() - mean_dark) / (mean_white - mean_dark)
113
114     # SPECTRAL SMOOTHING
115     # paulus technical refers to someone using 15, 3 on FX10
116     # spectral smoothing so on spectral axis
117     im_proc = savgol_filter(im_proc, 15, 3, axis=-1)
118
119     # discard start and end bands
120     im_proc = im_proc[:, :, 10:190]
121     # clip
122     im_proc = np.clip(im_proc, a_min=0, a_max=1)
123
124     #SEGMENTATION
125     # ratio vegetation index
126     # RVI = NIR / RED
127     RVI = im_proc[:, :, 150] / im_proc[:, :, 95]
128
129     # Determine threshold with Otsu's method
130     thresh = threshold_otsu(RVI)

```

```

131     mask = RVI > thresh *1.1
132
133     # Erode once with 5x5 elliptical kernel
134     kernel = cv2.getStructuringElement(cv2.MORPH_ELLIPSE,(5,5))
135     mask = cv2.erode(np.float32(mask), kernel, iterations=1)
136
137     # DIMENSIONALITY REDUCTION
138     # only calc pc on leaf pixels
139     leaf_px_idxs = np.nonzero(mask)
140     # extract leaf pixels found
141     leaf_px = im_proc[leaf_px_idxs[0], leaf_px_idxs[1], :]
142
143     # if none need to calculate pc
144     if pc is None:
145
146         # spectral principal components wants a 3D array
147         leaf_px = np.reshape(leaf_px, (1, -1, im_proc.shape[2]))
148
149         # find the pcs and create object to get the reduced feature set
150         pc = principal_components(leaf_px)
151         r = pc.reduce(num=n_features)
152         # TODO: experiment with best number of pcs
153
154         # do transform to im
155         reduced = np.absolute(r.transform(leaf_px))
156
157         # create dataset
158         sample_idxs = random.sample(range(len(leaf_px_idxs[0])), k=n_px)
159         X[i*n_px:(i+1)*n_px] = reduced[sample_idxs]
160         y[i*n_px:(i+1)*n_px] = scan['class'].value
161
162     # TRAIN CLASSIFIER
163     # split dataset into test and train partitions
164     # shuffle turned off since extraction is random and subslices are thus random
165     X_train, X_test, y_train, y_test = train_test_split( \
166         X, y, test_size=test_ratio, shuffle=False)
167
168     # setup classifier
169     clf = svm.SVC(decision_function_shape='ovo',
170                     kernel= 'rbf',
171                     C=20,
172                     gamma=0.2)
173
174     # train
175     clf.fit(X_train, y_train)

```

Chapter 6

System Validation

To verify and validate the overall system, an experiment was conducted. In the experiment, images were taken of plants grown with different treatments of fertiliser and microbes, resulting in different health of the plant. The system is verified by checking that it meets the specification to take pictures, process them, and analyse them. The system will be validated by assessing the ability to monitor the health of a plant.

6.1 Procedure

The potato plants used were grown in individual pots in a polytunnel at the University of Lincoln Riseholme Campus. The plants were of the same variety and grown in the same conditions but were given different treatments: fertiliser and microbial applications. The microbial treatment had two variations: microbes applied (YM) or not applied (NM) and the fertiliser application had 3 variations: no fertiliser (NF), basal fertiliser application (BF) and top dress fertiliser application (TD). If these variations are combined there are six different combinations of treatments given to the plants with five plants in each treatment group giving a total of 30 plants.

A visual health assessment of the plants was made, rating each either average, above average or below average. These were correlated with the plant's label, the result of which is displayed in Table 6.1. Observing this table, there is very little distinction in the effects of microbial treatment between the same fertiliser treatment, however, there does appear to be a clear trend in performance according to the fertiliser

treatments. For no fertiliser application, most plants are below average performance and for the basal fertiliser application, most plants are above average performance. For the top dress fertiliser application, no plants were below average performance but there was an even spread across average and above average performance. In the analysis, the initial goal will be to distinguish between the plants given no fertiliser against those with basal fertiliser and later other analyses will be incorporated.

Table 6.1: Table comparing the health assessment of each plant against its label.

Label	Performance Classification (count)		
	Below	Average	Above
NFYM	3	1	1
NFNM	4	1	0
TDYM	0	2	3
TDNM	0	3	2
BFYM	1	1	3
BFNM	0	0	5

As discussed earlier in this system, the cart was selected to be suitable for this particular imaging application and then the acquisition system was mounted to it. A photo of the plants and imaging system in use during testing can be seen in Figure 6.1.

The procedure for collecting the data, or operating the acquisition system, was as follows. After the system has been turned on and initialisation completed, the in-field calibration procedures are completed. Firstly the focus is set so that the plant canopy is in focus and checked that it is suitable for the variations in plant height between different pots. Next, the speed of the linear actuator is calibrated to ensure the aspect ratio is correct, then capture can begin. The cart is pushed up to a plant so that it will be in the frame of the camera. The illumination is set to the desired level. The scan number, plant number and other notable conditions are recorded. The button is pressed on the acquisition laptop to start scanning then after a moment the button is pressed to start the linear actuator moving. A brief pause is required to ensure several lines of the white reference panel are captured. Once the camera

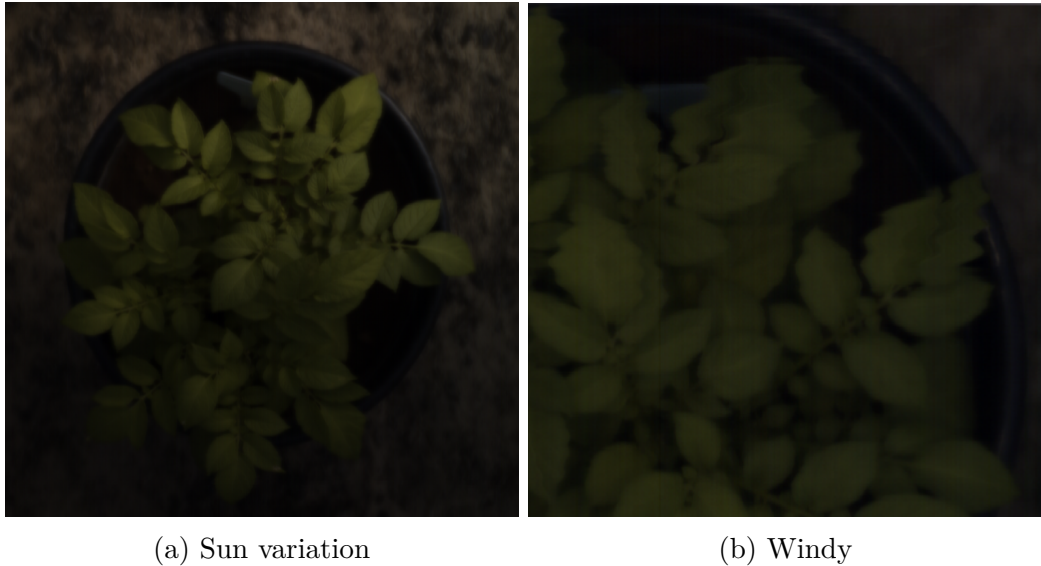


Figure 6.1: Photo of system during testing.

has captured the entire plant the stop button must be pressed on the acquisition laptop and the actuator will stop on its own then you can press the button to return to start and then repeat the procedure. If a notable event happened during the scan such as a wind gust or significant change in brightness, this was noted and decided if the event was significant enough to void the scan. Figure 6.2(a) shows an example of the change in illumination half way through the scan with the top half of the image brighter. Figure 6.2(b) shows the effects of wind during a scan with the plant moving as the camera captures the image, leading to spatial distortion.

6.2 Results

The data collection happened successfully at 2 pm during a day in August 2022, capturing images of all 30 plants with and without illumination. During the imaging the weather conditions were lightly cloudy and a slight breeze. The camera frame



(a) Sun variation

(b) Windy

Figure 6.2: Two types of imaging artefact that void a scan.

rate was 80 Hz, the exposure time was 7 ms and the linear actuator was calibrated to a speed of 44 mm s^{-1} .

Continuing to the processing subsystem, the details were specified in the relevant CSV file and then the data were fed through the correction and pre-processing pipeline that removed image variances and extracted features and samples for the machine learning. From each image, dimensionality was reduced to 7 features and 5000 pixels were sampled from each image with 20% reserved for the test partition.

The results of classifying No Fertiliser (NF) and Basal Fertiliser (BF) with no illumination are given in Figure 6.3. This two-class problem yielded an accuracy of 65% on the training set and 57% on the test set. Interestingly, the accuracy increases to 72% and 69% respectively for the same plants imaged on the same day with the artificial illumination at full. The confusion matrices are given in Figure 6.4. The finding that classification accuracy increases notably with the increased illumination is a significant find and should be used to inform the discussion around the illumination system.

The problem was extended to a three-class task by including the Top Dress (TD) variation of fertiliser treatment. The confusion matrices are given in Figure 6.5. The performance drops, as evidenced by the accuracy of approximately 50%. It is also

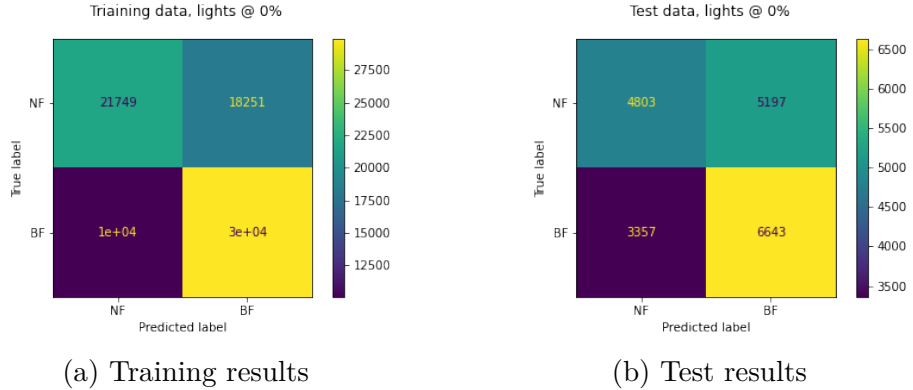


Figure 6.3: Confusion matrices for classification on classes NF and BF with no artificial illumination.

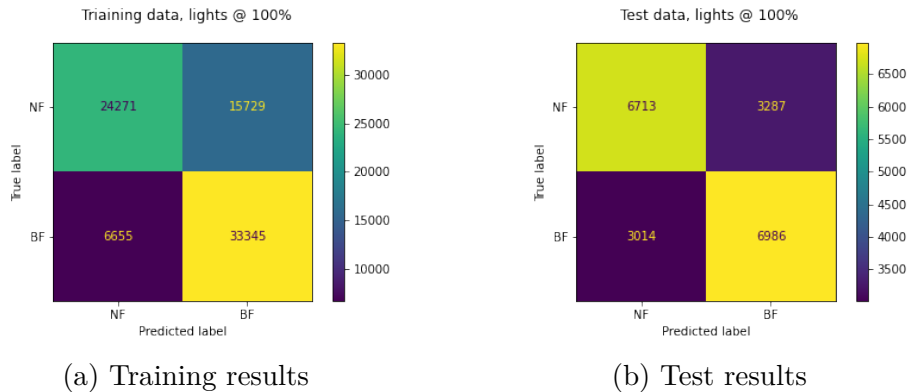


Figure 6.4: Confusion matrices for classification on classes NF and BF with artificial illumination set to full.

noteworthy that most of the confusion is between the two different applications of fertiliser and not the plants with no fertiliser applied.

These results show that the system is able to acquire and process hyperspectral images of plants such that their health can be monitored by predicting their health status with a classifier. There are areas for improvement which will be discussed in the following chapter.

Table 6.2: Table giving classification accuracy for different data configurations.

Classes	Light, %	Accuracy, %	
		Train	Test
NF, BF	0	64.7	57.2
NF, BF	100	72.0	68.5
NF, BF, TD	0	58.9	30.2
NF, BF, TD	100	50.2	48.9

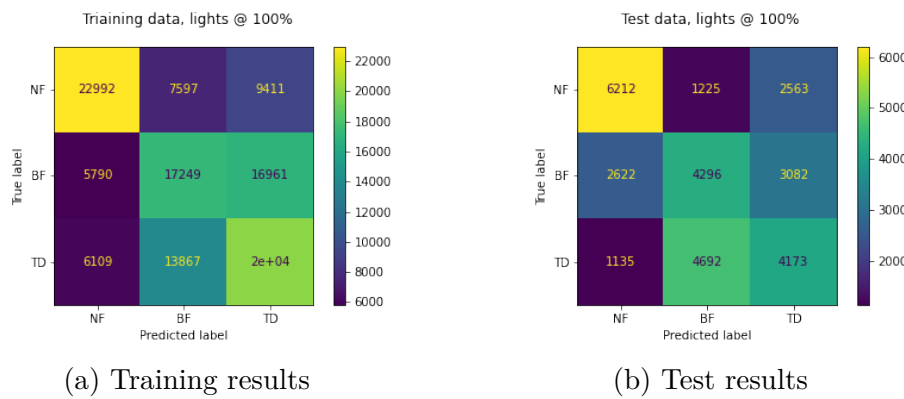


Figure 6.5: Confusion matrices for classification on classes NF, BF and TD with artificial illumination set to full.

Chapter 7

Discussion

7.1 Creating an automated acquisition system

The first project objective was to *create an automated acquisition system that will capture hyperspectral images of the plant's canopy* and has been accomplished to a high degree. The needs of the system were identified well through research and experimentation such as testing the camera system resulting in a good system design that integrated well. A challenge during the design of this aspect, and the entire project, was how to build something that would be versatile to different needs, environments and crops. The solution to modularise the system is a key aspect of this project where the linear actuator along with the accompanying components can be fitted to a cart suitable for the task at hand.

The hardware design of the actuator offers a design that performs well, is affordable and is low maintenance. The belt-driven solution is compact and lightweight and easy to implement and be controlled by the microcontroller. The electronics and firmware meet the system needs. Motion is smooth with the acceleration control implemented and the selection of the TMC stepper motor driver means the electronics stay cool and the silent operation aids in any reduction in vibration. The decision to select the ESP32 and use websockets to communicate with a web-based user interface is another success. This solution is elegant, very versatile and the graphical and interactive nature of the webpage makes the data collection process easy. A better solution would be to integrate the actuator control into the camera control, even incorporating lighting control too. The implementation of control in this project

was the best option given the constraints, but in future, a solution to combine the control into one interface is desirable, especially to aid in automating the process. Since the camera uses GigE, a common interface, different software or custom one could be used, alternatively, Lumo has a remote SDK that may be able to interface with.

The other significant aspect of the acquisition system that warrants discussion is illumination. Whilst natural illumination was sufficient to get reasonable results, the performance of the classifier was increased when artificial illumination was used, suggesting it was worthwhile to add artificial illumination into the scope of the project. The system wasn't trialled for classification in outdoor conditions or on a very bright day but the testing showed only 60% of the dynamic range of the camera would be utilised in such conditions. The obvious approach to increasing intensity is to increase the luminous output, however, due to the system being battery powered and there already being a significant power consumption from the illumination system another solution is desirable. The light is spread out over a much larger area than is required, thus, by concentrating it on the line, the intensity would be increased. Further to this, the uniformity of the light coverage has been an issue. The halogen reflector bulbs were found to have a central bright spot fading to the edge which not only led to non-uniformity but the lights were spread out so the bright spots didn't overlap which reduced overall intensity also. It is still believed that the array of multiple narrower reflector lamps as proposed will be challenging to get uniform. An alternative idea is to use the linear halogen bulbs because their light output is highly uniform and use a parabolic reflector with the lamp at the focal point so the light is focused into a parallel beam of light. This will concentrate the light onto a smaller area and by having parallel light, the issues encountered with the intensity reducing with distance should be mitigated. Although halogen lighting is widely regarded as the best broad band emitter it may be worth considering LED grow lights that claim to be a broad spectrum; they would have a significantly lower power consumption and avoid potential heat stress on the plant.

7.2 Developing a processing pipeline

The next objective was to *develop a processing pipeline to extract and fuse spectral and image-level features from the images for plant monitoring.* The pipeline developed performs well, reading images, removing the effect of varied lighting and filtering noise. There is some discrepancy in correcting for illumination but as discussed, that issue arises from a sub-optimal illumination system though there are measures that could be taken to correct for distance algorithmically.

The selection of spectral features works but it is an area that was not explored to its full extent in this project. Principal component analysis is common and effective but there may be better feature extraction methods or even a feature selection approach that is superior. Other methods to investigate could be successive projections algorithm or the partial least squares discriminant analysis. Another limitation of the approach taken to dimensionality reduction is that the features are only calculated on the first image the pipeline sees and then applied to all subsequent images. This may negate certain features in other images and an approach should be explored that handles this.

A further area that has been underutilised is image features. The current approach passes spectra of pixels to the classifier without an understanding of how they relate to each other. There is more information in these spatial relationships which is yet to be leveraged in this pipeline. In particular, textural features from co-occurrence matrices, grey level run length features or histogram features could be calculated and added as features to be passed to the classifier.

Finding the mask of the areas of vegetation performs well due to the vegetation index and Otsu's adaptive thresholding method. In these data the leaf coverage was good therefore stems being part of the mask was not an issue but other crops or different stages of maturity may pose other challenges. There are also other approaches that could be considered. When the plant flowers, the flowers could be studied separately, or even just their presence used. There are also several opportunities to do more advanced selection, for example, identifying leaves based on their maturity which

can be identified by certain spectral features and then passing this data in a grouped manner to the analysis so that features in leaves of certain maturity can be learnt.

7.3 Investigating algorithms for health classification

The third objective was to *investigate advanced machine learning algorithms for potato plant classification of health*. Advanced machine learning algorithms were implemented, yielding correct classifications for plant health. There is significantly more scope to investigate alternative machine learning algorithms, and potentially deep learning algorithms too. Adding to this is investigating the alternative spectral and image features as suggested in the previous section and the best algorithms for that.

This project has only focused on classification but an interesting extension and one which gets closer to a true score would be to turn this into a regression problem. It was decided to leave that outside the scope of this project due to the increased demands on data gathering and processing in limited timescales. This would require more data to be collected with more information about its health and work put into designing this aspect of the system to decide how a health score should be measured.

An aspect of the project that was planned but removed was time series data collection and analysis. This feature may be able to monitor individual plant growth to further aid in detecting changes to health and make predictions about their growth. This would also allow a better prediction of health to be made at different snapshot growth stages.

7.4 Validation of the system

The final objective was to *validate the system on potatoes grown in a polytunnel*. Validation of the system was successfully conducted by performing an experiment that captured images of different potato plants that were given different treatments

and classifying which plants were part of different treatment groups. On one hand, this provided a clear task that could be used to evaluate the system, however, the system was not tested to truly classify health, only the treatment group even though there is a strong correlation between each treatment and their health.

To further test the system, it needs to be tested in different growth stages of the plant and different varieties. It would also be beneficial to test the invariance to environmental factors by using images taken on different days and at different times of the day in the same dataset. To truly develop the system into a generalised automated health monitoring system, it should be tested on different crops and the level of automation increased.

7.5 Personal Reflection

This project has been a good opportunity to apply my existing skills to the new-to-me area of hyperspectral imaging and develop new ones along the way. The project required a lot of research to become familiar with the field of HSI and to understand the theories and technologies underpinning it such that I could develop a suitable solution. I believe that adopting a robust project methodology has helped to deliver this solution. The systems vee approach really helped to break a large complex problem down into constituent parts and then use SysML to study the connections between and within those parts. This helped to understand what the requirements for each subsystem were and consequently consider the feasibility so that the implementation was not embarked upon to later have to redesign or rescope the system.

I feel risks were managed well throughout the project. For example, I regularly monitored the growth of the potatoes and when they were showing signs of failure contingency plans were shored up to scan alternative plants in the walled garden and another polytunnel. Eventually, the crop I planned to image for salt stress did fail due to the temperatures in the polytunnel, but there was negligible impact on the project due to the contingency plans. One risk I did not manage as well was the workshop availability which caused some tasks to take longer. I was in discussions

about the project with the engineering workshop from an early stage but I failed to confirm the head of the workshop's availability and learnt with only a few days notice that they were on annual leave for a whole month. This impacted this project with a lack of support and being unable to access the facilities on some days but, fortunately, hasn't impacted the final outcome significantly.

On one hand, I think the project has suffered from not devoting more time to the analysis but due to the way the project was designed it was necessary to build the acquisition system first and it turns out it was very good to add artificial illumination to the scope. In reflection, it was in the best interest of the project to do it this way and the extra analysis elements are there for further work. An alternative would have been to only focus on the analysis and use an existing dataset but the interplay of acquisition and processing is interesting and necessary to build an optimal solution. I would not have learnt as much about the different aspects of HSI if not for adopting that approach. This is evidenced by designing the illumination system. Upon initial testing, there were some improvements to be made but ultimately it lit the area, however, the full extent of the effect of illumination was only revealed during the processing. The underutilised dynamic range and understanding that because of the height placement of the reference panel and the nature of the light made the correction underperform. From this, it has been possible to suggest further improvements to the design of the illumination system.

Chapter 8

Conclusions

The goal of this project was to develop an automated hyperspectral imaging system for monitoring plant status, in particular, moving towards in-situ, in-field imaging. Evaluating against the objectives, an acquisition system was created that uses the Specim FX10 hyperspectral line scanning camera which is moved by a custom-built linear actuator using a timing belt and stepper motor controlled by a microcontroller. The images are acquired using Specim Lumo Recorder and the actuator is controlled by a webpage that is hosted on the microcontroller. This system is designed to be used to image the plants in situ which means there is varying natural illumination that must be accounted for. An artificial illumination system was built using halogen reflector bulbs that move with the camera to increase the light intensity as required by hyperspectral imaging. The illumination system does aid imaging but there are improvements to be made, including increasing the intensity by concentrating the light on a smaller area and improving uniformity. A notable feature of the acquisition system is that it is modular such that it can be mounted to different frames depending on the imaging application.

A processing pipeline was built in Python that prepares the data for analysis. The image is made invariant to varying lighting conditions by retrieving reflectance values with the aid of a white reference panel in every image. The data is prepared for analysis by extracting pixels from the image using the ratio vegetation index and reducing the dimensionality using principal component analysis. There is scope to investigate alternative feature selection methods in further work and to include image features obtained from spatial information such as textural features. The analysis

uses a support vector machine classifier to estimate the health of each plant. There is further scope to explore a regression problem to achieve a continuous health score and how health is defined, to expand the analysis to a time series problem, and to investigate other machine learning methods.

The system was validated on potatoes grown in pots in a polytunnel which were given different treatments. The classifier was able to distinguish between plants that were given fertiliser and those that hadn't with 68.5% accuracy on the test partition. The next steps for this project is to act on the further work and publish the system as an open source integration of the hardware and software processing elements.

References

- Aghaei, Keyvan, Ali Akbar Ehsanpour and Setsuko Komatsu (2008). ‘Proteome Analysis of Potato under Salt Stress’. In: *Journal of Proteome Research* 7.11. PMID: 18855355, pp. 4858–4868. DOI: 10.1021/pr800460y. eprint: <https://doi.org/10.1021/pr800460y>. URL: <https://doi.org/10.1021/pr800460y> (cit. on p. 4).
- Couture, JJ et al. (2018). ‘Integrating spectroscopy with potato disease management’. In: *Plant disease* 102.11, pp. 2233–2240 (cit. on p. 5).
- Duckett, Tom et al. (2018). ‘Agricultural Robotics: The Future of Robotic Agriculture’. In: ISSN: 2398-4422. DOI: 10.31256/WP2018.2 (cit. on p. 2).
- Gates, David M et al. (1965). ‘Spectral properties of plants’. In: *Applied optics* 4.1, pp. 11–20 (cit. on p. 4).
- Gerhards, Max et al. (2016). ‘Water stress detection in potato plants using leaf temperature, emissivity, and reflectance’. In: *International journal of applied Earth observation and geoinformation* 53, pp. 27–39 (cit. on p. 5).
- Gold, Kaitlin M et al. (2020). ‘Hyperspectral measurements enable pre-symptomatic detection and differentiation of contrasting physiological effects of late blight and early blight in potato’. In: *Remote Sensing* 12.2, p. 286 (cit. on p. 5).
- Guiñón, José Luis et al. (2007). ‘Moving average and Savitzki-Golay smoothing filters using Mathcad’. In: *Papers ICEE 2007*, pp. 1–4 (cit. on p. 11).
- Halley, Richard John and Richard J Soffe (2003). *Primrose McConnell’s The Agricultural Notebook*. 20th ed. Blackwell Publishing (cit. on p. 4).
- Khan, Muhammad Jaleed et al. (2018). ‘Modern Trends in Hyperspectral Image Analysis: A Review’. In: DOI: 10.1109/ACCESS.2018.2812999. URL: http://www.ieee.org/publications_standards/publications/rights/index.html (cit. on p. 3).
- Lightbulbs Direct (2022). *Halogen Light Bulbs*. URL: <https://www.lightbulbs-direct.com/light-bulbs/halogen/> (visited on 15th Sept. 2022) (cit. on p. 32).
- Lu, Guolan and Baowei Fei (Jan. 2014). ‘Medical hyperspectral imaging: a review’. In: *Journal of Biomedical Optics* 19 (1), p. 010901. ISSN: 1083-3668. DOI: 10.1117/1.JBO.19.1.010901 (cit. on p. 3).

- Mishra, Puneet, Mohd Shahrimie Mohd Asaari et al. (2017). ‘Close range hyperspectral imaging of plants: A review’. In: *Biosystems Engineering* 164, pp. 49–67 (cit. on pp. 4, 5, 8, 11, 12).
- Mishra, Puneet, Menno Sytsma et al. (2022). ‘All-in-one: A spectral imaging laboratory system for standardised automated image acquisition and real-time spectral model deployment’. In: *Analytica Chimica Acta* 1190, p. 339235 (cit. on pp. 8, 10).
- Morales, Alejandro et al. (2022). ‘Laboratory Hyperspectral Image Acquisition System Setup and Validation’. In: *Sensors* 22.6, p. 2159 (cit. on pp. 6–8, 10).
- Ooznest Limited (n.d.). *NEMA17 Belt Driven Linear Actuator Test Data*. Available at <https://ooznest.co.uk/wp-content/uploads/2018/06/NEMA17-Belt-Driven-Linear-Actuator-Test-Data.pdf> (07/05/22) (cit. on pp. 7, 36).
- Paulus, Stefan and Anne-Katrin Mahlein (2020). ‘Technical workflows for hyperspectral plant image assessment and processing on the greenhouse and laboratory scale’. In: *GigaScience* 9.8, giaa090 (cit. on pp. 4, 6–8, 10–12, 47).
- Roper, Jenna M., Jose F. Garcia and Hideaki Tsutsui (Mar. 2021). ‘Emerging Technologies for Monitoring Plant Health in Vivo’. In: *ACS Omega* 6 (8), pp. 5101–5107. ISSN: 24701343. DOI: 10.1021/acsomega.0c05850 (cit. on p. 2).
- Roy, Manojit et al. (2000). ‘Simple denoising algorithm using wavelet transform’. In: *arXiv preprint nlin/0002028* (cit. on p. 11).
- Sarić, Rijad et al. (Mar. 2022). ‘Applications of hyperspectral imaging in plant phenotyping’. In: *Trends in Plant Science* 27 (3), pp. 301–315. ISSN: 1360-1385. DOI: 10.1016/J.TPLANTS.2021.12.003 (cit. on p. 3).
- Serranti, Silvia, Aldo Gargiulo and Giuseppe Bonifazi (2011). ‘Characterization of post-consumer polyolefin wastes by hyperspectral imaging for quality control in recycling processes’. In: *Waste Management* 31 (11), pp. 2217–2227 (cit. on p. 3).
- Specim (n.d.). *Smile and Keystone*. Available at <https://www.specim.fi/smile-and-keystone/> (07/05/22) (cit. on pp. 8, 9).
- Superior Lighting (2022). *How To Choose Your Halogen Light Bulb*. URL: <https://www.superiorlighting.com/lighting-resources/light-bulb-learning-center/halogen-light-bulbs/how-to-choose-your-halogen-light-bulb/> (visited on 15th Sept. 2022) (cit. on p. 32).
- Van De Vijver, Ruben et al. (2020). ‘In-field detection of Alternaria solani in potato crops using hyperspectral imaging’. In: *Computers and Electronics in Agriculture* 168, p. 105106 (cit. on pp. 5, 7, 8).
- Yuen, P W T and Mark Richardson (2010). ‘An introduction to hyperspectral imaging and its application for security, surveillance and target acquisition’. In: *The Imaging Science Journal* 58 (5), pp. 241–253 (cit. on p. 3).

Zhang, Yanchao et al. (2019). ‘Automated spectral feature extraction from hyper-spectral images to differentiate weedy rice and barnyard grass from a rice crop’. In: *Computers and Electronics in Agriculture* 159, pp. 42–49 (cit. on pp. 7, 8, 11, 12).